AD-A070 292 ROYAL AIRCRAFT ESTABLISHMENT FARNBOROUGH (ENGLAND) F/G 20/4
A THEORETICAL STUDY OF THE SUPERCRITICAL AEROFOIL NLR 7301, AND--ETC(U)
SEP 78 R C LOCK

UNCLASSIFIED RAE-TR-78119 DRIC-BR-78119 NL

| OF |
AD
A070292

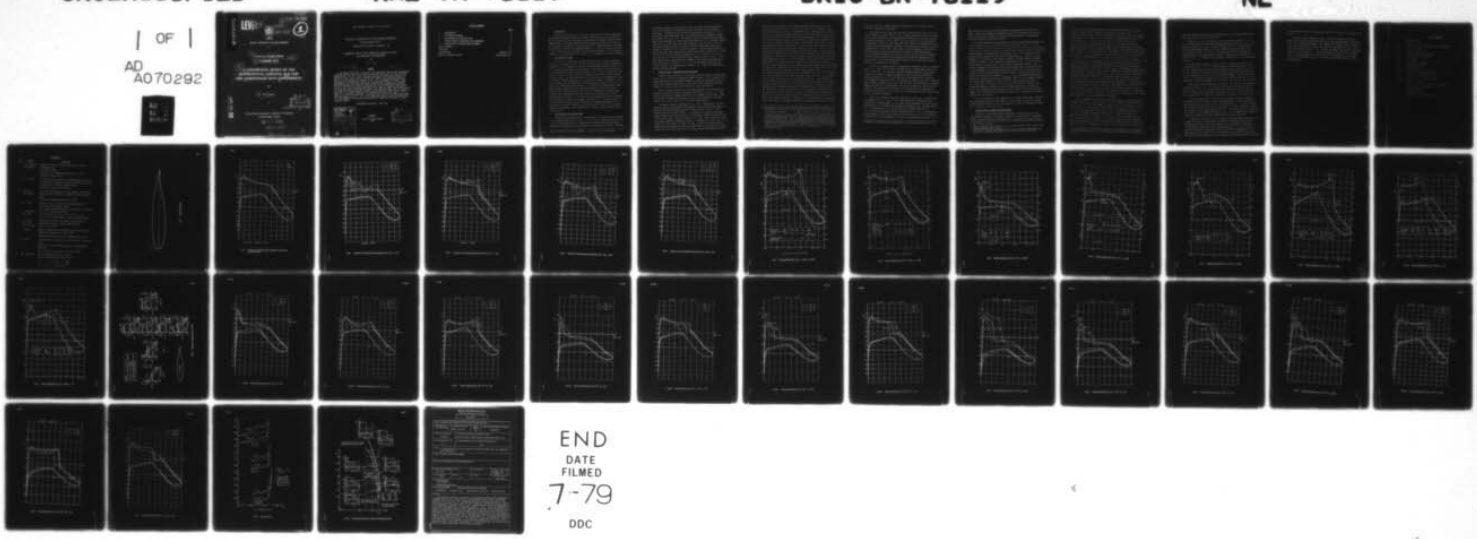

END
DATE
FILMED
7-79
DDC

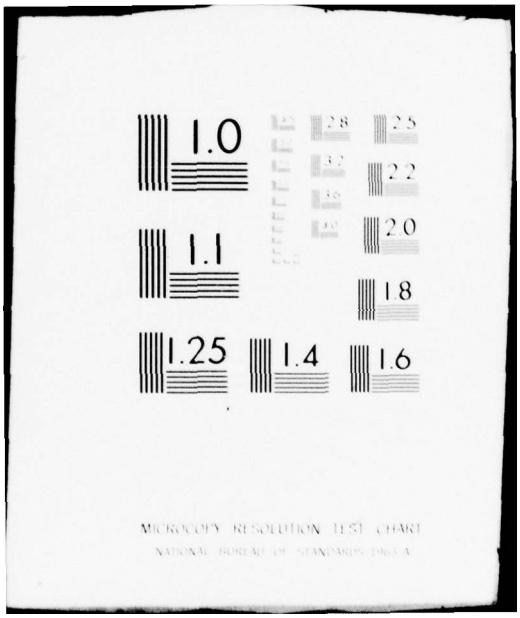
1.0
1.1
1.25
1.4
1.6
2.8
3.2
3.6
4.0
2.5
2.2
2.0
1.8
MICROCOPY RESOLUTION TEST CHART
NATIONAL BUREAU OF STANDARDS 1963-A

(14) RAE – TR-78119

LEVEL II

(18) DRIC

(19) BR-78119

1

NW

ROYAL AIRCRAFT ESTABLISHMENT

*

(9) Technical Report 78119

(11) September 1978

(12) 45p.

(6)

A THEORETICAL STUDY OF THE SUPERCRITICAL AEROFOIL NLR 7301, AND COMPARISON WITH EXPERIMENTS.

by

(10) R.C. Lock

*

Procurement Executive, Ministry of Defence
Farnborough, Hants

UNLIMITED

UDC 533.693.9 : 533.6.011.35 : 533.6.071

ROYAL AIRCRAFT ESTABLISHMENT

Technical Report 78119

Received for printing 27 September 1978

A THEORETICAL STUDY OF THE SUPERCRITICAL AEROFOIL NLR 7301, AND COMPARISON WITH EXPERIMENTS

by

R. C. Lock

SUMMARY

The aerofoil NLR 7301, 16.5% thick, was designed at NLR by their generalised hodograph method to give supercritical (inviscid) shock-free flow at the design condition $M_\infty = 0.72$, $C_L = 0.6$. The paper describes a theoretical study of this aerofoil by the latest form of the RAE 'VGK' method for calculating viscous effects in two-dimensional transonic flows. First, comparisons are given with experiments in the NLR Pilot Tunnel at a low Reynolds number (2×10^6). Large discrepancies are shown near the design condition and at higher Mach numbers, which are ascribed to a laminar (transitional) shock wave/boundary layer interaction in the transition-free experiments; this causes an apparent weakening of the shock wave and a spuriously low level of the measured drag. Next, calculations were made at two higher Reynolds numbers, with transition fixed near the leading edge: 10^7, to simulate conditions in a medium-sized wind tunnel; and 5×10^7, typical of full-scale conditions. Favourable scale effects are predicted on drag-rise Mach numbers, for $C_L > 0.5$, and on separation onset at all lift coefficients. It is concluded that the aerofoil should have an excellent performance at high Reynolds numbers.

Departmental Reference: Aero 3444

LIST OF CONTENTS

1 INTRODUCTION

The aerofoil NLR 7301 is a 16.5% thick supercritical aerofoil, designed by the generalised hodograph method of Boerstoel and Huizing[1]; it was selected by NLR for inclusion in the 'data base' of experimental information supplied to the AGARD FDP WG4. The present Report describes an extensive theoretical study of this aerofoil by the method of Collyer[2] and Lock[3,9]; comparisons with experiments in the NLR Pilot Tunnel (at a Reynolds number of 2×10^6) are included, but most of the calculations have been made at higher Reynolds numbers - 10^7 to represent conditions in a larger wind tunnel, and 5×10^7 to represent full scale conditions.

2 THE NUMERICAL METHOD

The method of calculation, described briefly in Ref 4 (p 469) and fully in Ref 2, is an adaption of the inviscid finite difference method of Garabedian and Korn[5] (G & K), combining it with the 'lag-entrainment' method of Green *et al*[6] for calculating the boundary layer and wake to allow fully for viscous effects; the 'transpiration' model of the displacement effect is used to provide an inner boundary condition for the inviscid calculations, both on the aerofoil surface and in the wake. The method has been recently improved by incorporating a variant of Jameson's[7] 'quasi-conservative' (Q-C) difference scheme; a parameter λ has been introduced in the 'shock-point' difference operator which is such that $\lambda = 0$ gives a non-conservative (N-C) scheme, $\lambda = 1$ gives the Q-C scheme, while intermediate values naturally lead to intermediate results. Since it has been generally noted that neither the 'N-C' or 'Q-C' extremes give uniformly good agreement with experiment (when viscous effects are allowed for), it is not surprising that a value of λ of about 0.5 does generally give better agreement with experiment: see Ref 3 for example. This value of λ has been used in all the calculations described below. Otherwise the standard parameters of the method have been used*: results are all for the 'fine' (160 × 30) grid, making normally 50 iterations on the 'coarse' (80 × 15) grid followed by about 200 on the fine grid.

3 CALCULATIONS FOR INVISCID FLOW

The aerofoil is shown in Fig 1. Calculations of the pressure distribution for the design condition ($M_\infty = 0.721$, $\alpha = -0.2^\circ$, $C_L = 0.599$) are shown in Fig 2; the full line being the 'exact' (shock-free) solution obtained by the design method and the dashed line that obtained by the present direct method. Agreement

---

* The 'artificial viscosity' parameter ε (EP) is set at 0.8 throughout.

is excellent except near the rear sonic point, and there the shock predicted by the direct method is so weak that a drag coefficient of only 0.00016 is calculated. Fig 3a&b show how the pressure distribution develops at $\alpha = -0.20$ as the free stream Mach number (M_∞) is increased from 0.68 through the design Mach number (0.72) up to 0.73. As expected a shock of moderate strength appear near the leading edge ($M_\infty = 0.68$) which moves back as M_∞ is increased, growing weaker while a second (also weak) shock appears at $\frac{x}{c} \triangleq 0.6$ ($M_\infty = 0.715$). At the design condition these two coalesce to form one weak shock, which grows rapidly in strength as M_∞ is further increased. A rather similar pattern is seen in Fig 4a&b, which show how the presence distribution varies with α (from -0.5° to $+0.1^\circ$) at the design Mach number (0.72). As is usual with a supercritical aerofoil of this type, quite small changes in either M_∞ or α from their design values came appreciable changes in the pressure distribution, but Fig 5 shows that for values of α or M_∞ *below* the design values the drag 'creep' is small, not exceeding about 0.0005 in C_D. Above the design point, the drag increases rapidly.

4 VISCOUS THEORY: COMPARISONS WITH EXPERIMENT

A model of the aerofoil, of 0.18 m chord, has been tested in the NLR Pilot tunnel (0.55 m × 0.42 m) at a Reynolds number of about 2×10^6. Because of the low Reynolds number, the dilemma of whether to test with transition 'fixed' or 'free' was more acute than usual; in fact tests of both types have been made, though as we shall see later each type has its particular defects.

First, we note from Fig 6 the very large reduction in lift predicted by allowing for viscous effects at the design condition ($M_\infty = 0.72$, $\alpha = -0.2^\circ$); the lift coefficient is reduced from 0.6 to 0.3, almost exactly halved. (Here, the position of transition was taken to be at the suction peak on the upper surface ($x/c \triangleq 0.07$), and at $x/c = 0.3$ on the lower surface.)

We consider next the combination of M_∞ and α which appears at first sight to lead to an experimental distribution (transition free) most similar to that for the inviscid design condition. This is at $M_\infty = 0.747$, $\alpha = 0.85^\circ$ (uncorrected) and is shown in Fig 7. In an endeavour to obtain a good match between viscous theory and experiment, the following procedure has been used in this and other cases. First the presence ratio p/H_∞ over the first 20% chord on the upper surface is matched by varying α, keeping M_∞ fixed. Next M_∞ is varied: as is well known, the values of p/H_∞ on the *upper* surface near the leading edge suction peak are almost invariant with M_∞ when the flow is supercritical so that a match with the *lower* surface pressure distribution over the

front part of the aerofoil can be obtained without disturbing that already achieved on the upper surface. In fact, the value of M_∞ arrived at in this way was found to be very close to the nominal value, suggesting that no blockage correction is required: somewhat surprising in view of the rather large (10%) open area ratio of the slotted walls, which would suggest that a negative blockage correction might be needed. The position of transition was specified to be as far back as possible on both surfaces. On the upper surface this is at the suction peak just before the shock ($x/c = 0.58$); on the lower surface it proved impossible to get the transition point further aft than $x/c = 0.37$*. In this way very good agreement with experiment over the front third of the aerofoil is achieved; but further aft the situation is very different. The most noticeable discrepancy is on the upper surface: here theory suggests that there should be a marked shock wave at $x/c \triangleq 0.6$, strong enough to cause about 40 'counts' of wave drag; while in the experiment there is apparently no shock at all. What has almost certainly happened is that a laminar shock-wave/boundary-layer interaction has taken place, which has smeared out the pressure rise through the shock to such an extent that it has become quite smooth. This phenomenon has also caused the wave drag associated with the shock to be negligible: the value of C_D measured (by a pitot transverse in the wake 0.8 chords downstream of the trailing edge) is only 0.0084 as opposed to the calculated value 0.0123. It is significant that the purely 'viscous' part of the calculated drag (*i.e.* neglecting wave drag) is 0.0082, agreeing closely with the experimental value. Making the reasonable assumption that transition from laminar to turbulent flow is taking place in the experiment at about the position ($x/c = 0.6$) assumed in the calculations, we can deduce that little wave drag is present in the experimental measurements; whereas the calculations suggest that there would be about 40 'counts' of wave drag if the boundary layer were turbulent at its interaction with the shock wave. On the lower surface, agreement between theory and experiment is better, though

---

* The reason for this is that Thwaites' method, which is used to calculate the laminar part of the boundary layer, breaks down (indicating a laminar separation) when the parameter $-\lambda = -\frac{\theta^2}{\nu}\frac{dU}{dx}$ exceeds the critical value 0.08. If a transition point is specified such that this critical value is reached, then the program automatically moves the transition position forward until a non-critical situation occurs. This may easily happen when the specified position is far back on the chord, even in an apparently favourable pressure gradient, because the disturbance to the pressure distribution at transition may induce a local *adverse* gradient sufficient to trigger the process (θ being relatively large, so that only a small value of dU/dx is needed to cause λ to reach its critical value).

there are signs of a laminar separation bubble near x/c = 0.5 which cannot of course be predicted by the theory.

The results for the same case, but with transition fixed at x/c = 0.3 on both surfaces, are shown in Fig 8. With a normal calculation (full line) having these transition positions, the agreement with experiment on the upper surface is again poor behind x/c = 0.3, while over the rear part of the lower surface the measured pressures are much lower than those predicted, suggesting that the roughness band has thickened the boundary layer sufficiently to bring it near to separation at about 70% chord. Some support to this hypothesis is provided by some additional calculations made with an increment in momentum thickness ($\Delta\theta_{tr}$) artificially added at the transition point (on both surfaces), shown by the dashed lines; clearly the pressures are now nearer the measured ones on both surfaces. Note that a double shock pattern occurs on the upper surface, which is not predicted by the theory.

Figs 9 to 12 compare theory with experiment (transition free) at a constant value of α (0.85°) in the latter, through the set of Mach number values 0.6, 0.7, 0.72 and 0.77. At the three lower Mach numbers agreement is quite good, except in the region of laminar separation on the lower surface mentioned previously, and also over the last 10% chord on the upper surface, where the present method is usually found to overestimate the pressure rise to the trailing-edge slightly. However at $M_{\infty} \triangleq 0.774$ (Fig 12) there are again signs of a marked laminar interaction in the experiment. [It was not possible to reach this Mach number in the calculations; even at $M_{\infty} = 0.765$, boundary layer separation is predicted from the foot of the shock to the trailing edge, while at higher values of M_{∞} the method diverged.]

Figs 13 to 15 compare results at constant M_{∞} (0.745) as α_T varies from -2° through 0° to $+2^{\circ}$. At $\alpha_T = -2^{\circ}$ we have chosen the 'transition fixed' conditions in the experiment. On the upper surface agreement is good but on the lower surface it is probable that separation is imminent (note the high value of $\bar{H}$, 2.2, predicted at x/c = 0.8), provoked by the strong shock wave at x/c = 0.45 and the subsequent adverse pressure gradient. At $\alpha_T = 0$ (transition free) agreement is fair on both surfaces (Fig 14); but at $\alpha_T = +2^{\circ}$ (transition fixed) (Fig 15) it was impossible* to reach a sufficiently high value of α in

---

* Because the calculations diverged (owing to excessively high values of $\bar{H}$).

the calculations to match with the experimental pressures over the first 25% chord - even so the agreement is moderately good on both surfaces and in particular it is clear that a laminar interaction has been avoided in the experiment by fixing transition ahead of the shock.

Our final comparison with experiment is in Fig 16, which shows measured and predicted values of C_D for the 'transition free' condition with $\alpha_T = 0.85^o$ (taking the position of transition in the calculations as far back on the chord as the method will allow*; as marked in the appropriate figures). It will be seen that the theory slightly overestimates the drag from $M_\infty = 0.6$ to 0.7 (usually for other aerofoils, with transition fixed near the leading edge, it is found[9] to *underestimate* C_D by about the same amount). However, *the most marked discrepancy* is that the 'bucket' in the experimental measurements at $M_\infty = 0.747$ is replaced in the theory by a rapid rise in drag at about the same Mach number. This strongly suggests that the laminar shock wave/boundary layer interaction present in the experiment is producing unrealistically low** values of the drag, particularly at the higher Mach numbers *where the shock is far back along the chord.* Note also the dotted curve marked '$C_{D\ viscous}$' (twice the momentum thickness calculated at 'infinity' downstream in the wake). This *does* have a marked 'bucket', due to the rapid movement of transition on the upper surface, back from $x/c = 0.09$ at $M_\infty = 0.72$ (Fig 11) to 0.6 at $M_\infty = 0.745$ (Fig 7). Without this *transition movement, the value of the total* drag coefficient calculated at $M_\infty = 0.745$ would have been much higher, by about 0.004; so that drag-rise Mach number, M_D, would have been predicted as about 0.73, as opposed to the apparent value of 0.75 from Fig 16.

A pictorial summary of the comparisons of pressure (Mach number) distribution is provided by Fig 17, which gives on a small scale a 'traverse' through the Mach number range 0.6 to 0.77 at constant $\alpha_T = 0.85^o$, and through the range of α from -2^o to $+2^o$ at $M_\infty = 0.745$.

5 CALCULATIONS AT HIGHER REYNOLDS NUMBERS

Because of certain unsatisfactory features, referred to above, of the experimental information at present† available for this aerofoil - unavoidable at the low Reynolds number of the NLR tests - it was decided to make a purely

---

* See footnote on page 5

19 ** In the sense that they would not occur in fully turbulent flow, even at high Reynolds numbers (see section 5).

† The aerofoil has now been tested in the Lockheed Georgia Compressible Flow facility at high Reynolds numbers, but results are not yet available.

theoretical study of its behaviour at two higher Reynolds numbers: 10^7, being typical of what would be obtainable in a larger wind tunnel, and 5×10^7, a typical full-scale value. The present method was used, with transition fixed at 0.03 chord on both surfaces. First 'traverses' in Mach number were made at constant values of C_L = 0.3, 0.4, 0.5, 0.55 (Re = 10^7 only), 0.6 and 0.65 (Re = 5×10^7 only) - starting in each case at M_∞ = 0.6 and increasing in sufficiently small steps to enable the drag rise Mach number (M_D) and the Mach numbers for onset of trailing edge separation (M_{sep}) to be determined with reasonable accuracy. The former (M_D) is here conventionally defined to be the value of M_∞ for which C_D is 0.0020 greater than its value at M_∞ = 0.6 at the same lift coefficient: except that for $C_L > 0.5$ there is some wave drag (*ie* $C_{D\ total} > C_{D\ viscous}$), so that $C_{D\ viscous}$ at M_∞ = 0.6 has then been used as the datum value. The latter (M_{sep}) has been estimated by using the empirical observation that appreciable effects of trailing edge separation (in particular, divergence of trailing edge pressure) are found in practice when the transformed boundary layer shape parameter $\bar{H}$ exceeds about 2.2* one boundary layer thickness upstream of the trailing edge on the upper surface, ($\bar{H}_{1-\delta} > 2.2$). Next, in order to extend the estimated 'separation boundaries' to lower Mach numbers and higher lift coefficients, traverses in α at constant values of M_∞ were made, increasing α until separation conditions were obtained, as defined above. It was found however that this procedure was only satisfactory at Mach numbers of 0.72 and 0.70; for lower values of M_∞ the shock waves became so strong that excessive values of $\bar{H}$ (> 2.5) were predicted at the foot of the shock well before $\bar{H}_{1-\delta}$ reached the critical value. In such circumstances the prediction of separation must be treated with reservation in our present state of knowledge.

Before examining the predictions of M_D and M_{sep}, we show some typical pressure distributions. First, for Re = 10^7, Fig 18a,b&c show the results for C_L = 0.4, for M_∞ from 0.6 through 0.74 (M_D) up to 0.76 (beyond M_{sep}). Similar curves for C_L = 0.5 are shown in Fig 19a&b ($M_D \triangleq 0.73$, $M_{sep} \triangleq 0.74$), and for C_L = 0.6 in Fig 20a&b ($M_D \triangleq 0.65$, $M_{sep} \triangleq 0.73$). Corresponding drag curves, for C_L = 0.4, 0.5 and 0.6, are shown later in Fig 26. Fig 21 shows how the pressure distribution varies with C_L for M_∞ = 0.65; at the highest value of C_L, 1.02, separation is predicted at the trailing edge but would undoubtedly have occurred earlier at the foot of the shock. Temporarily, this situation can lead in practice to an appreciable *increase* in lift coefficient, as long as the

* It is important to note that this particular value should only be associated with the present method: it is not intended to imply any absolute significance to it.

separation bubble does not reach the trailing edge; so that the predicted value for $C_{L_{sep}}$ may not in fact be optimistic.

Turning now to the calculations at full-scale Reynolds number (5×10^7), we show in Fig 22a&b how the pressure distribution varies with M_∞ at $C_L = 0.6$; and in Fig 23a&b at $C_L = 0.65$. At first sight the effect of the increase in Reynolds number appears small; but a close comparison of Figs 20b [$Re = 10^7$, $C_L = 0.6$] and 22b [$Re = 5 \times 10^7$, $C_L = 0.6$] shows that the shock strength is slightly weaker at the higher Reynolds number. Some pressure distributions at $M_\infty = 0.72$ with C_L increasing up to separation conditions ($C_L \triangleq 0.83$) are shown in Fig 24.

An interesting comparison is made in Fig 25, in which are shown at the 'design point' ($M_\infty = 0.72$, $C_L = 0.6$) the pressure distributions at $Re = 10^7$ and 5×10^7, compared with the shock-free distribution given by the full line. At $Re = 10^7$ a shock is present sufficiently strong to cause appreciable wave drag (so that this point is well beyond the drag-rise boundary - see Fig 27); but at $Re = 5 \times 10^7$ the shock is weaker and in fact this condition turns out to be an optimum one (giving the maximum value of ML/D) at full scale for this aerofoil.

Some typical curves showing the variation of C_D with M_∞ at constant C_L are shown in Fig 26. At $C_L = 0.4$ there is little scale effect on either drag creep or M_D. At $C_L = 0.5$ there is much less drag creep full-scale than at $Re = 10^7$, though M_D is not greatly affected. But at $C_L = 0.6$ the drag creep is so large at $Re = 10^7$ that M_D is only 0.64, as opposed to 0.725 at $Re = 5 \times 10^7$.

The final figure, Fig 27, gives the drag rise and separation boundaries estimated for this aerofoil at the two Reynolds numbers. As mentioned above, a strong favourable scale effect on M_D is predicted for $C_L > 0.5$; and as regards the separation boundary the effect is favourable at all lift coefficients (above 0.4), though it does increase further with C_L. Thus under full-scale conditions, the aerofoil at its optimum condition $M_\infty = 0.72$, $C_L = 0.6$ should have a margin to separation of about 0.02 in Mach number and 0.23 in lift coefficient.

We have also included in Fig 27 sketches of the Mach number distribution at a number of points on the drag-rise and separation boundaries (full-scale), showing how the shape of the curves varies over a wide range of conditions. It is interesting to note that, at the optimum point ($M_\infty = 0.72$, $C_L = 0.6$), the pressure distribution corresponds closely to Whitcomb's recommendations[10] for a good supercritical aerofoil, with a weak expansion just behind the shock wave:
119 but with the added advantage of a more 'peaky' upper surface pressure distribution,

with appreciable isentropic compression (from $M \triangleq 1.3$ to about 1.2) ahead of the shock.

Thus the aerofoil shows every sign of being an extremely good one in practice; but as we have mentioned earlier the existing experimental information about it is extremely misleading. For example Fig 16 would indicate a value of M_D of about 0.755 (at $C_L = 0.45$); this point has been marked on Fig 27, and it can be seen that this value of M_D is about 0.02 higher than the value predicted *full-scale* for the same C_L. It must be emphasised that this does *not* appear to be a blockage problem: it is entirely due to the suppression of the shock wave at the low Reynolds number of the tests by interaction with the laminar boundary layer.

LIST OF SYMBOLS

c	aerofoil chord
C_D	drag coefficient
C_{D_V}	theoretical viscous drag coefficient (from wake)
C_L	lift coefficient
C_p	pressure coefficient
H	boundary layer shape parameter
H_∞	free stream total pressure
M	Mach number
M_∞	free stream Mach number
M_D	drag rise Mach number
p	static pressure
Re(R)	Reynolds number (based on chord)
V	velocity at edge of boundary layer
x,y	Cartesian coordinates (see Fig 1)
X_T(XT)	value of x/c at transition point
α	angle of incidence
α_T	angle of incidence in wind tunnel (uncorrected)
ϵ	artificial viscosity parameter
λ	shock parameter
ν	kinematic viscosity
θ	boundary layer momentum thickness

REFERENCES

No.	Author	Title, etc
1	J.W. Boerstoel G.H. Huizing	Transonic shock-free aerofoil design by an analytic hodograph method. AIAA 74-539 (1974) See also: Proc. Symposium Transsonicum II, p 109 (Springer Verlag, 1976)
2	M.R. Collyer	An extension to the method of Garabedian and Korn for the calculation of transonic flow past an aerofoil to include the effects of a boundary layer and wake. RAE Technical Report 77104 (1977)
3	R.C. Lock M.R. Collyer	A note on the prediction of viscous effects on aerofoils, with particular reference to transonic flows with shock waves. RAE Technical Memorandum Aero 1735 (1977)
4	R.C. Lock	Research in the UK on finite difference methods for computing steady transonic flows. Proc. Symposium Transsonicum II, p 469 (Springer Verlag, 1976)
5	P. Garabedian D.G. Korn	Analysis of transonic aerofoils. Com. Pure Appl. Math, 24, p 841 (1971). See also: Supercritical Wing Sections, I and II (Springer Verlag)
6	J.E. Green D.J. Weeks J.W.F. Brooman	Prediction of turbulent boundary layers and wakes in compressible flow by a lag-entrainment method. ARC R & M 3791 (1977)
7	A. Jameson	Numerical computation of transonic flows with shockwaves. Symposium Transsonicum II, p 384 (1976)
8	-	Unpublished NLR data supplied to AGARD FDP WG 4 (1977)
9	R.C. Lock	The prediction of viscous effects on aerofoils in transonic flow. Paper given at DGLR Symposium 'Transonic Configurations', June 1977. Also RAE Technical Memorandum Aero 1780 (1978)
10	R.T. Whitcomb	Review of NASA supercritical airfoils. 9th ICAS Conference Paper 74/10 (1974)

Fig 14

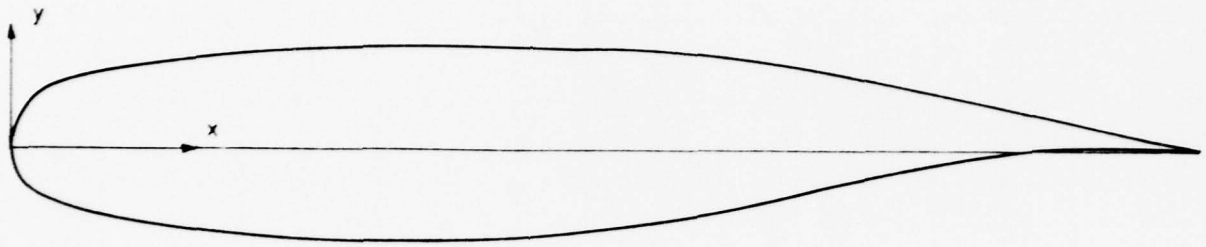

Fig 1 NLR 7301 Aerofoil

Fig 2

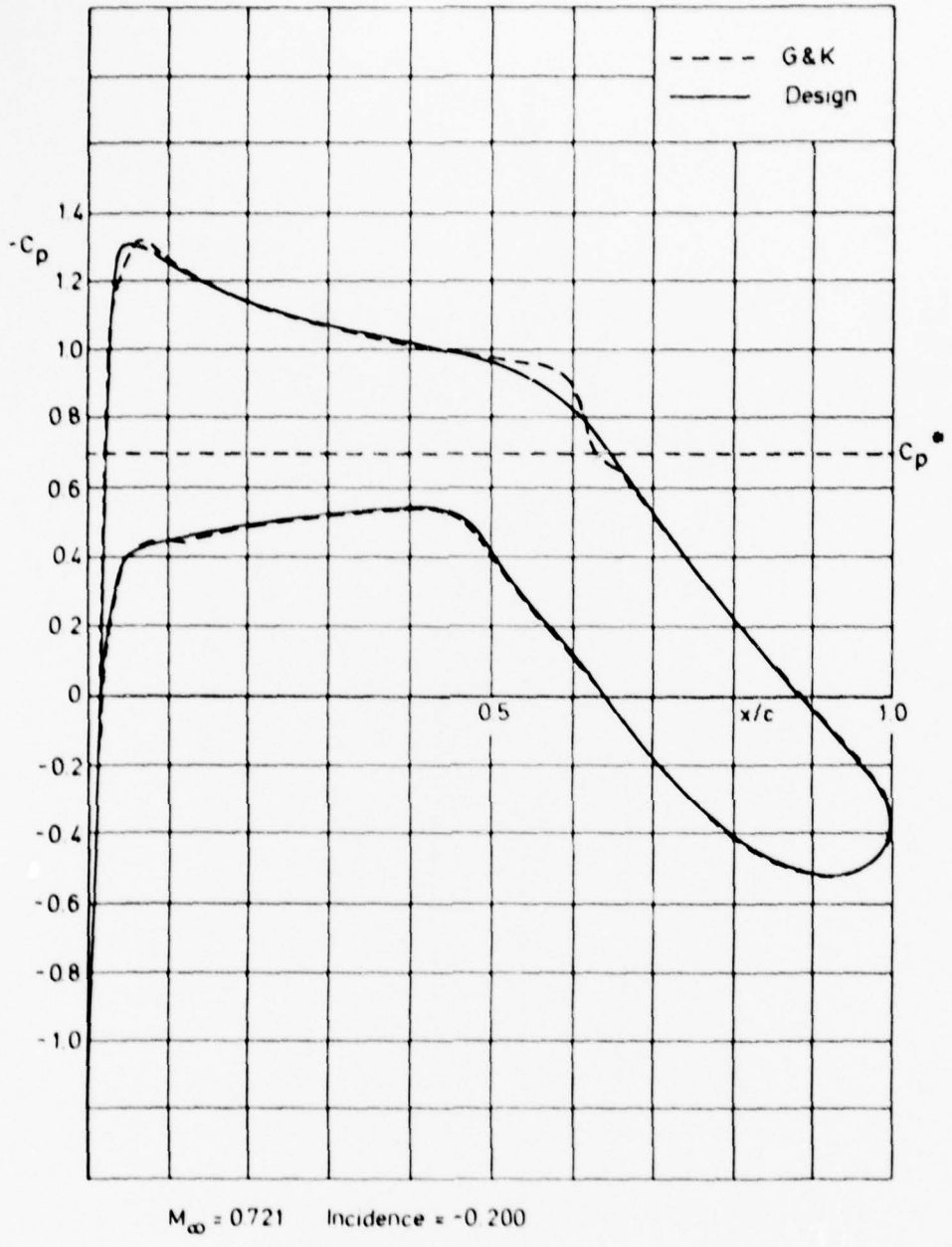

Fig 2 Comparison of design pressure distribution with a direct inviscid calculation

TR 78119

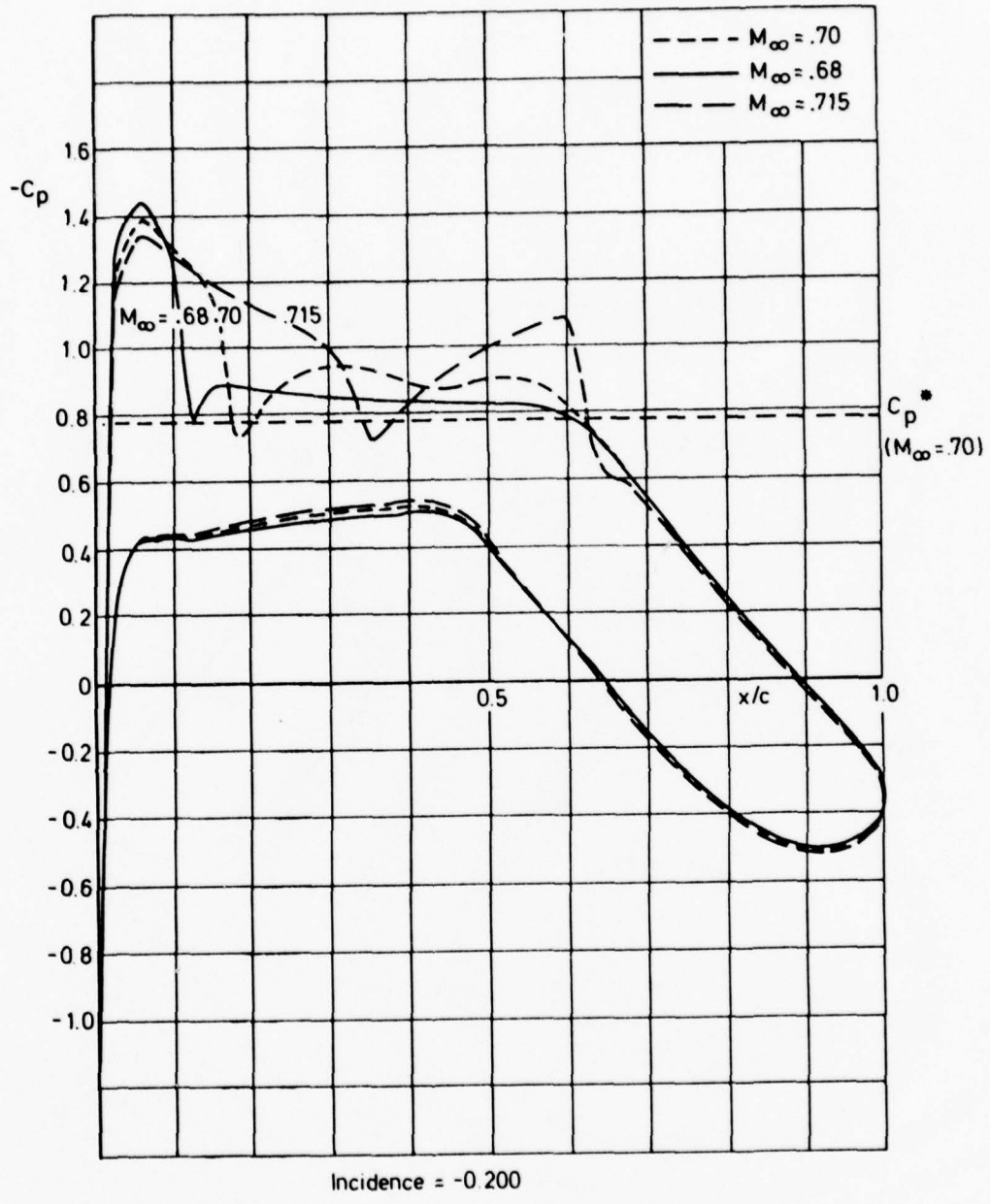

Fig 3a Variation of inviscid pressure distribution with M_∞ ($\alpha = -0.2°$)

TR 78119

Fig 3b

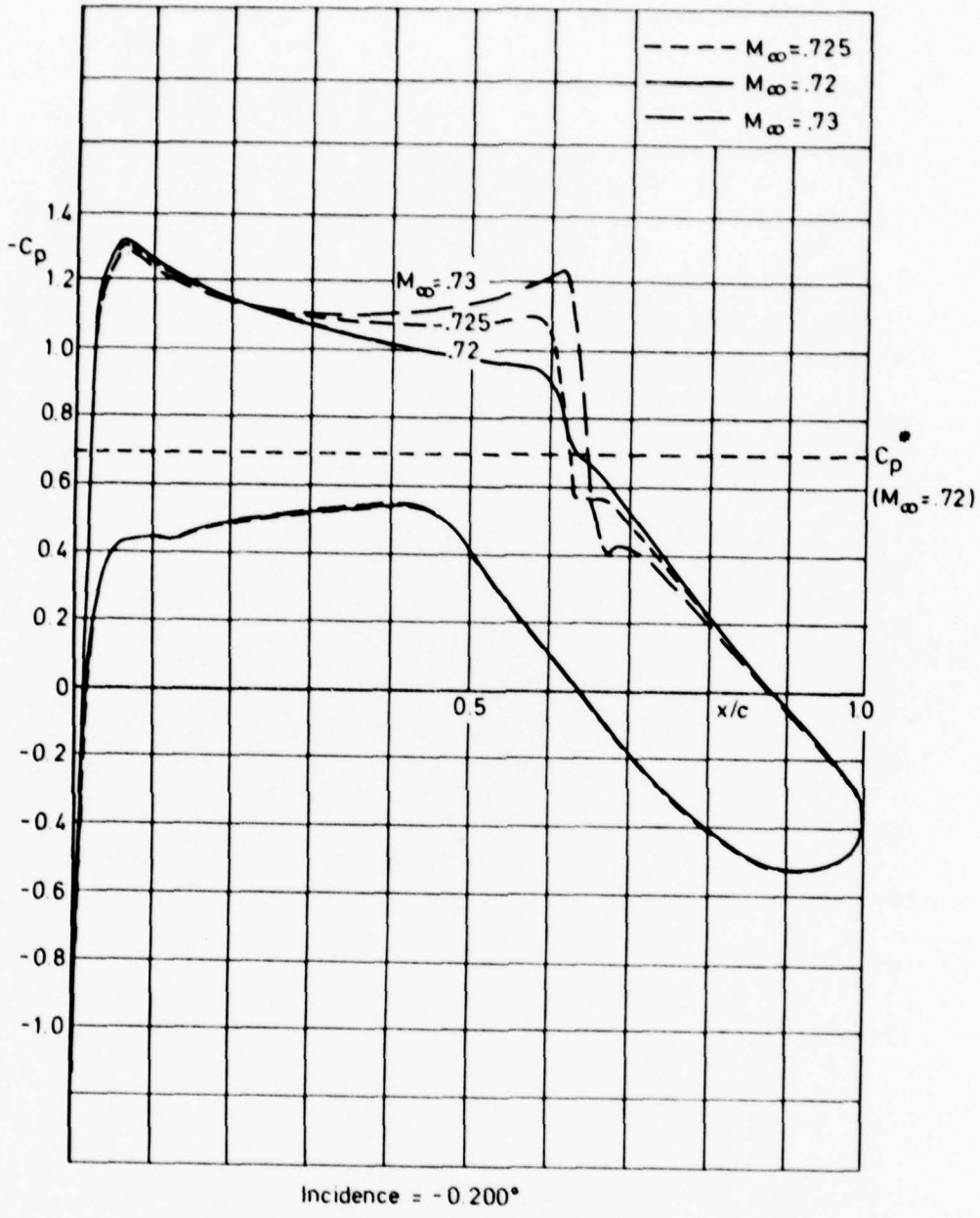

Fig 3b Variation of inviscid pressure distribution with M_∞ ($\alpha = -0.2°$)

TR 78119

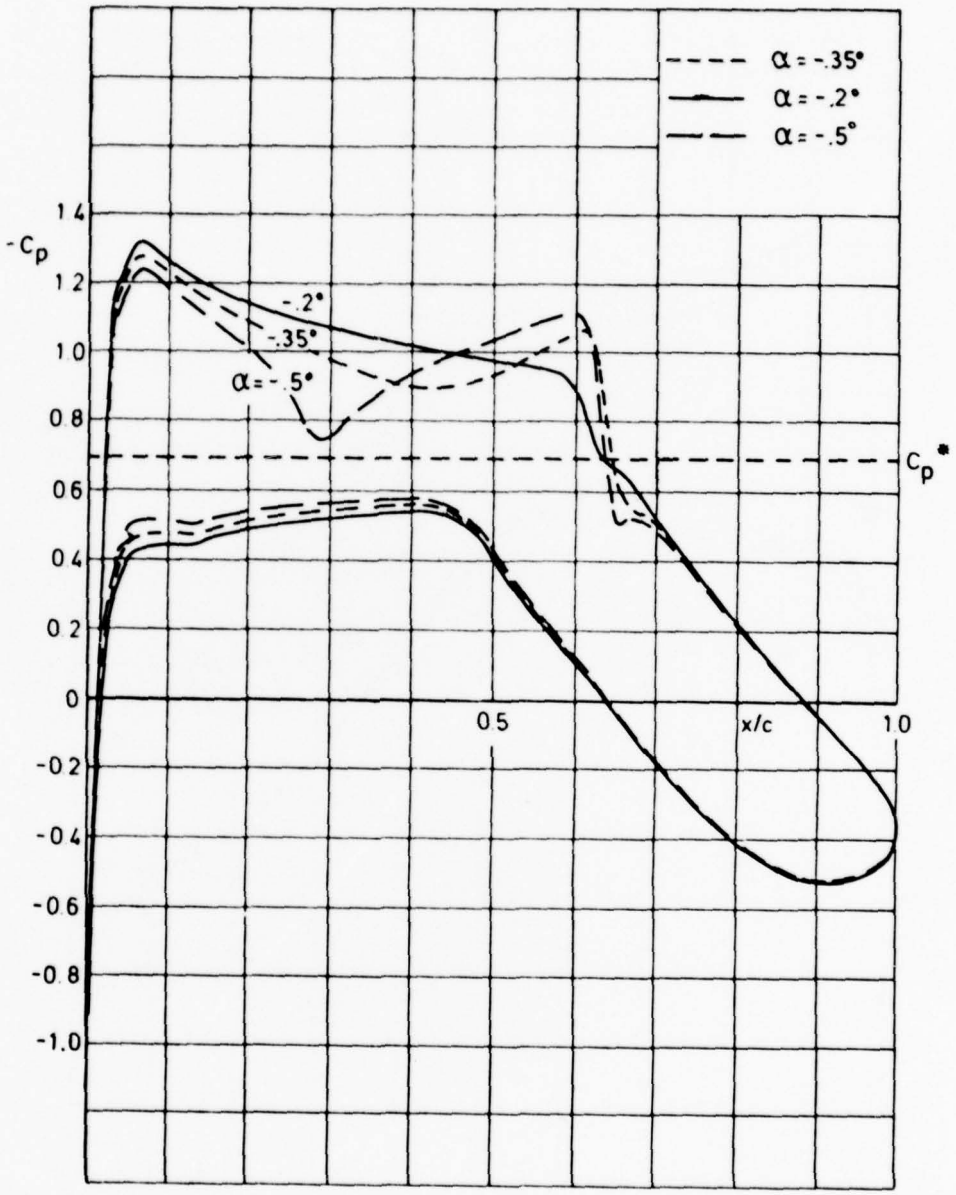

Fig 4a Variation of inviscid pressure distribution with α ($M_\infty = 0.72$)

TR 78119

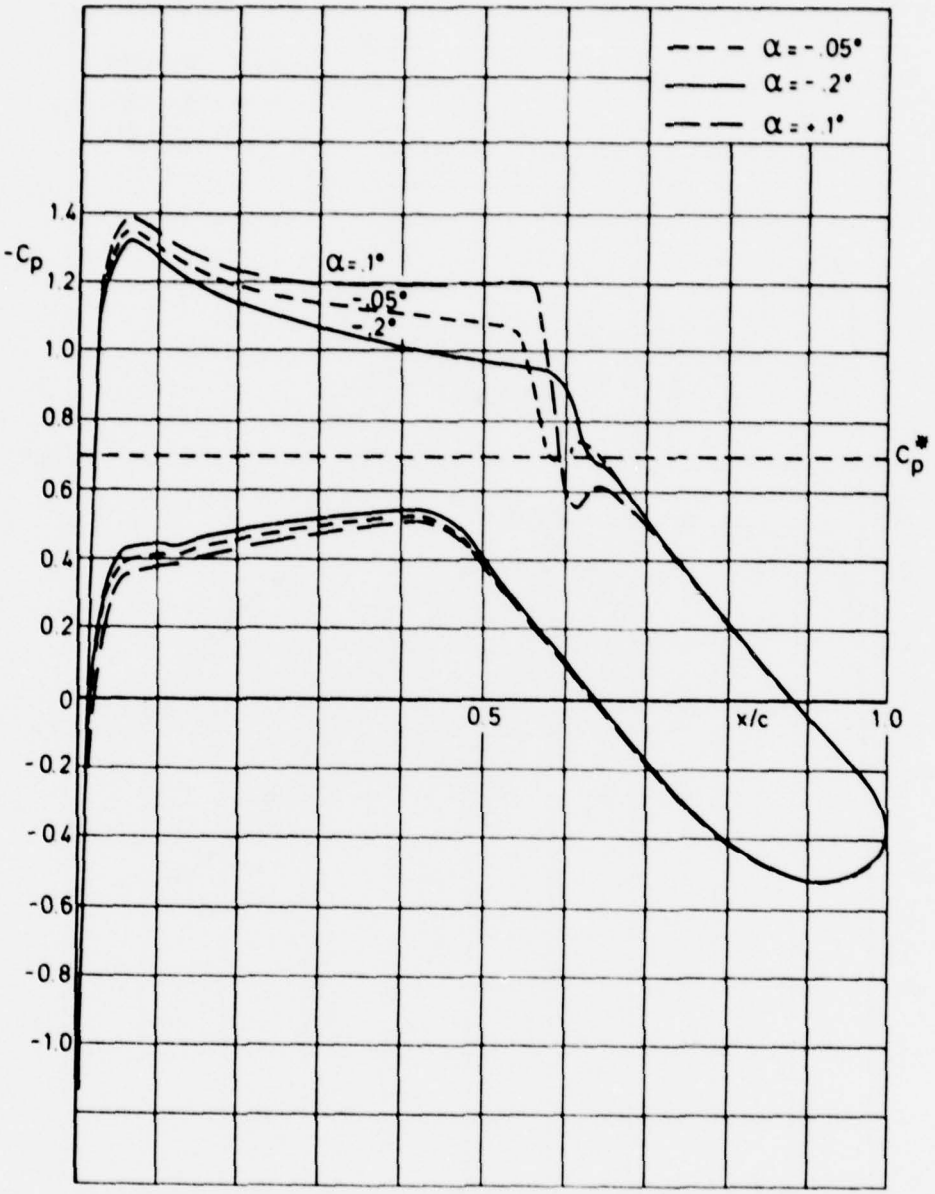

Fig 4b Variation of inviscid pressure distribution with α (M_∞ = 0.72)

TR 78119

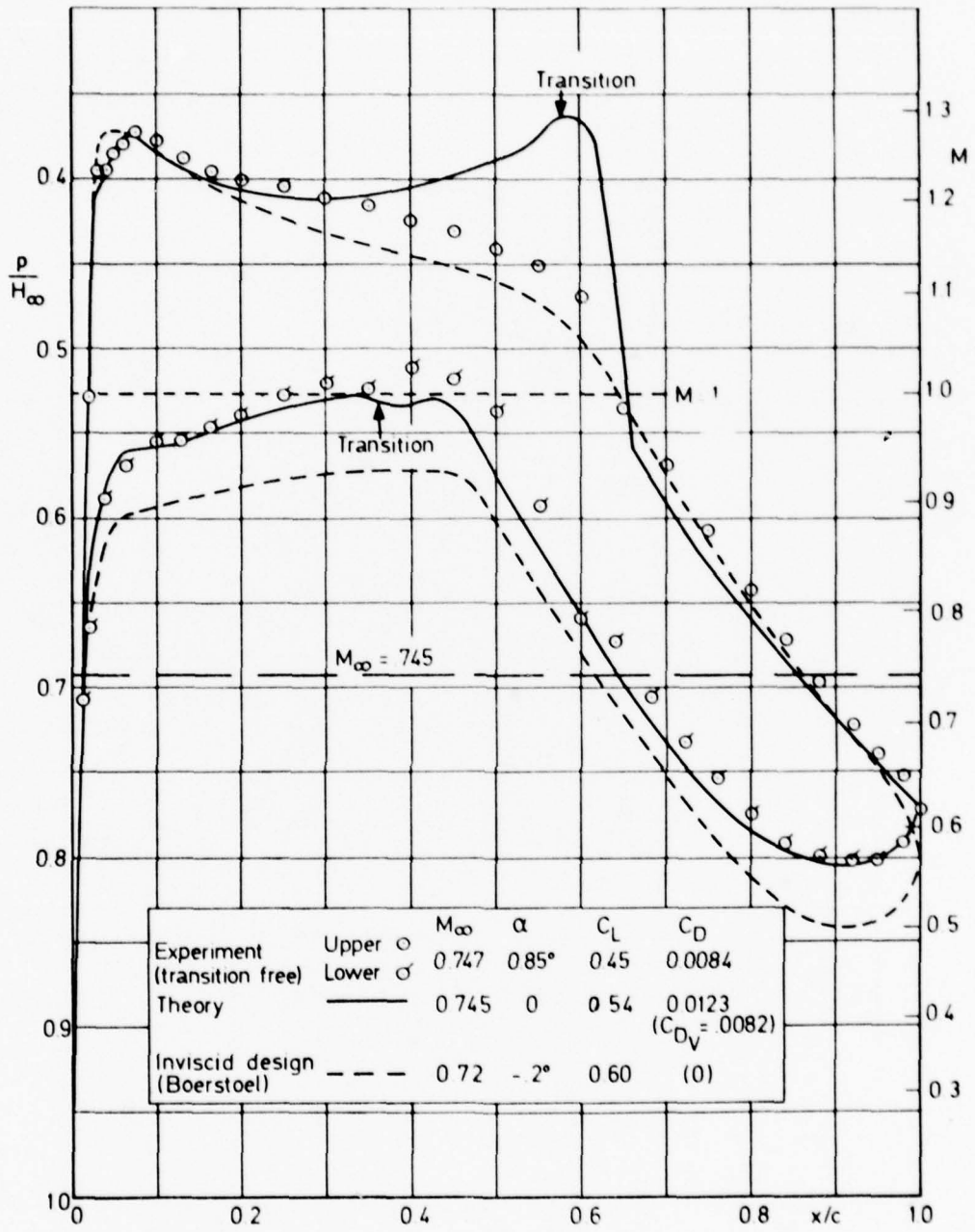

Transition free : $Re \triangleq 2 \times 10^6$

Fig 7 Pressure distributions at $M_\infty \triangleq 0.745$, $\alpha_T = 0.85°$

TR 78119

Fig 8

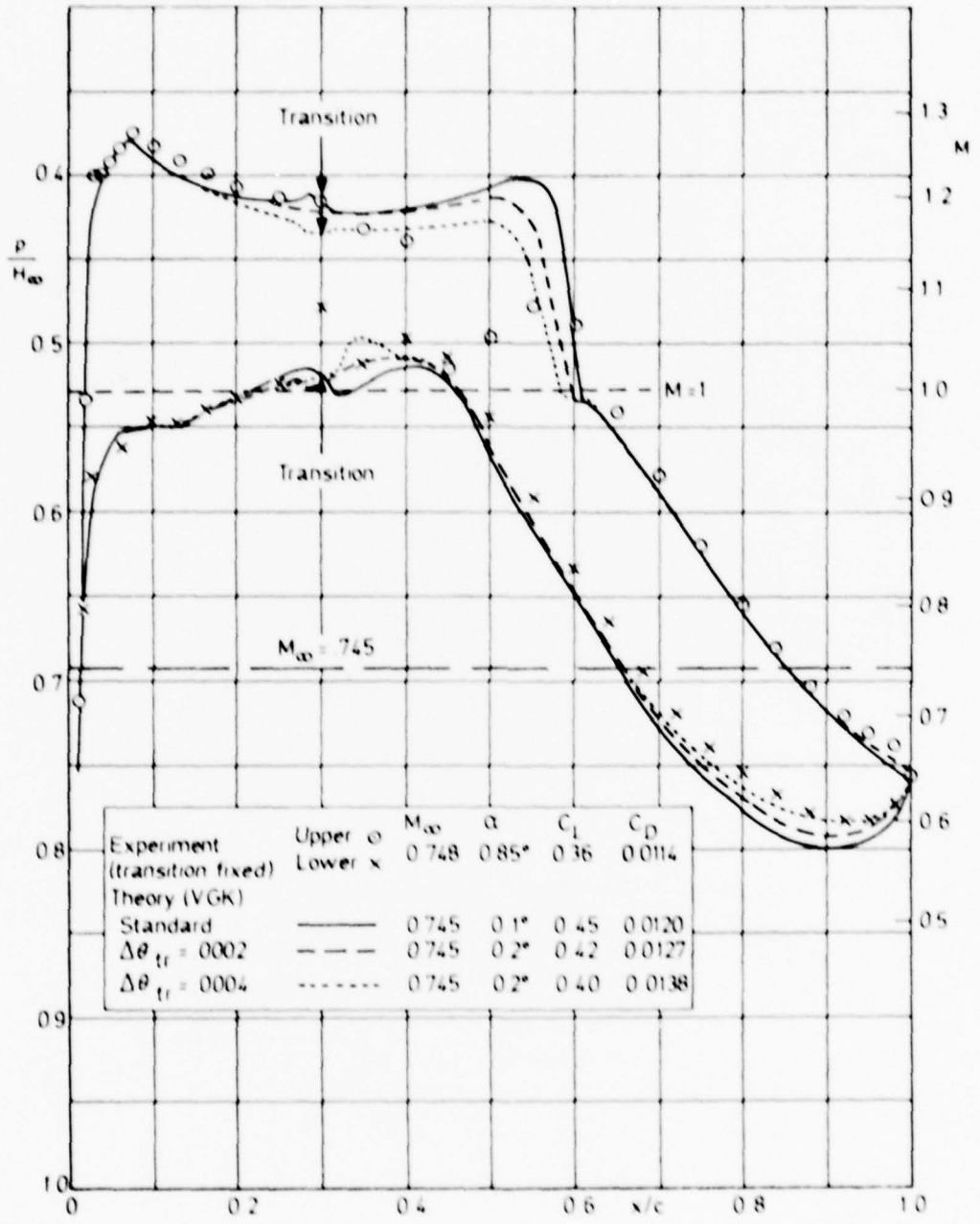

Transition fixed : $Re \triangleq 2 \times 10^6$

Fig 8 Pressure distributions at M_∞ = 0.745, α_T = 0.85°

TR 78119

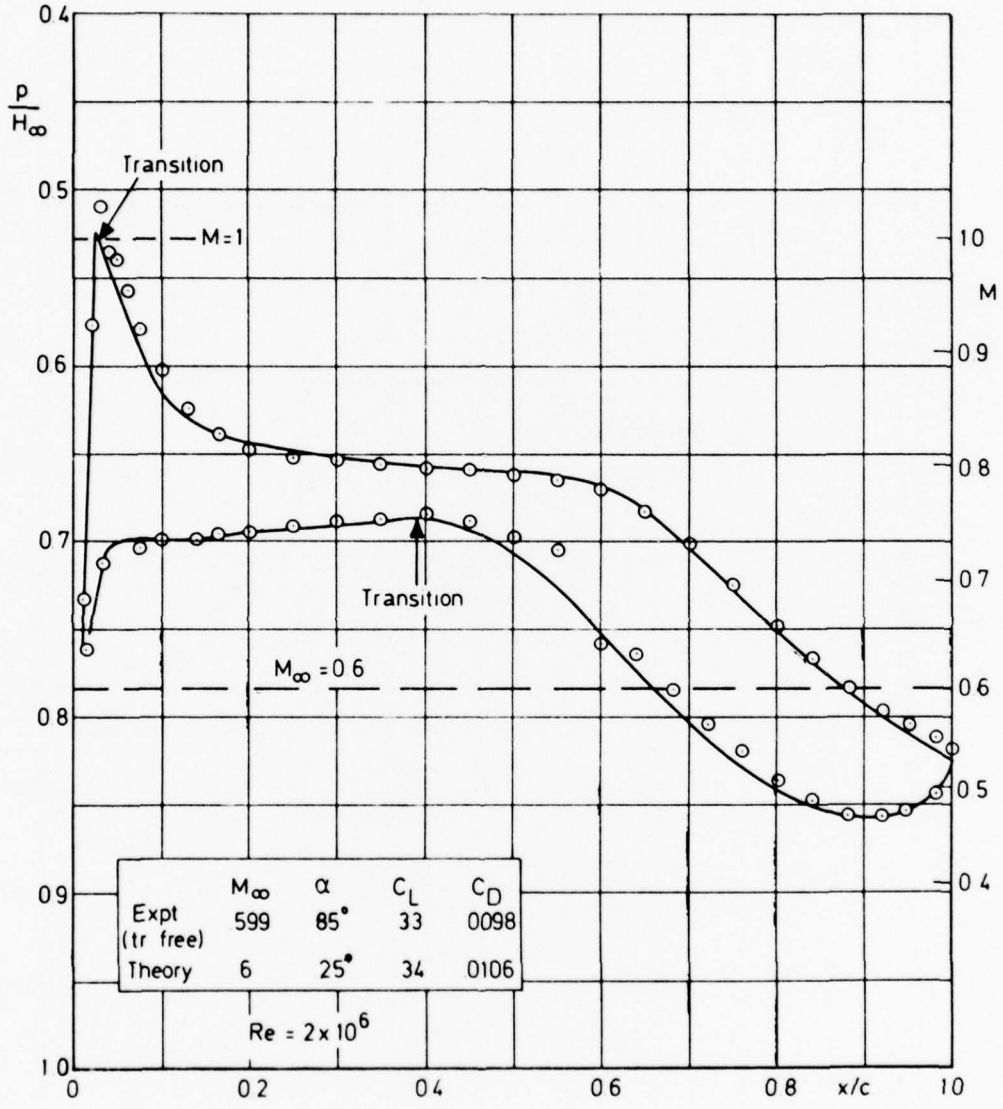

Fig 9 Pressure distributions at $M_\infty = 0.6$, $\alpha_T = 0.85°$

Fig 10

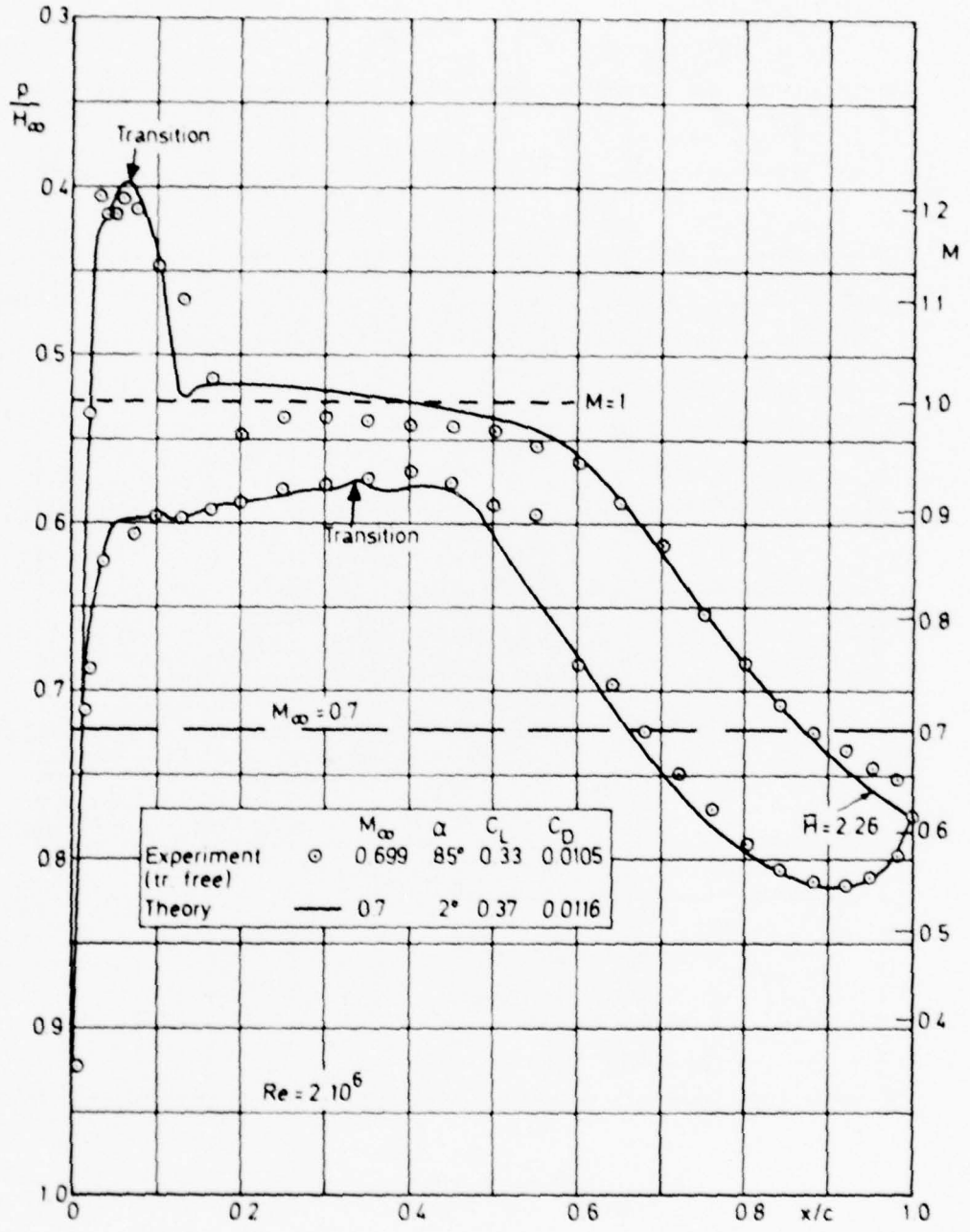

Fig 10 Pressure distributions at $M_\infty = 0.7$, $\alpha_T = 0.85°$

TR 78119

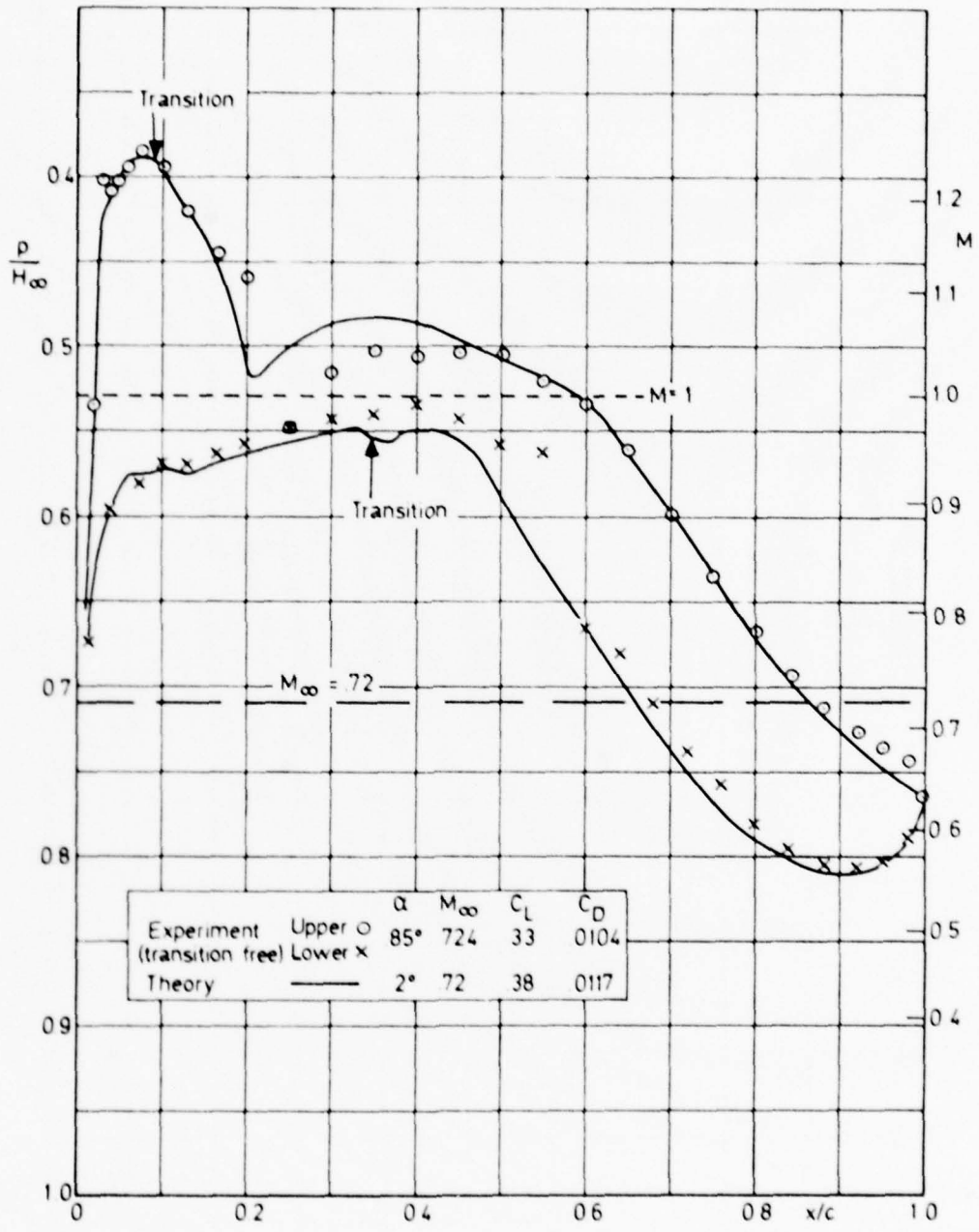

Fig 11 Pressure distributions at $M_\infty = 0.72$, $\alpha_T = 0.85°$

Fig 12

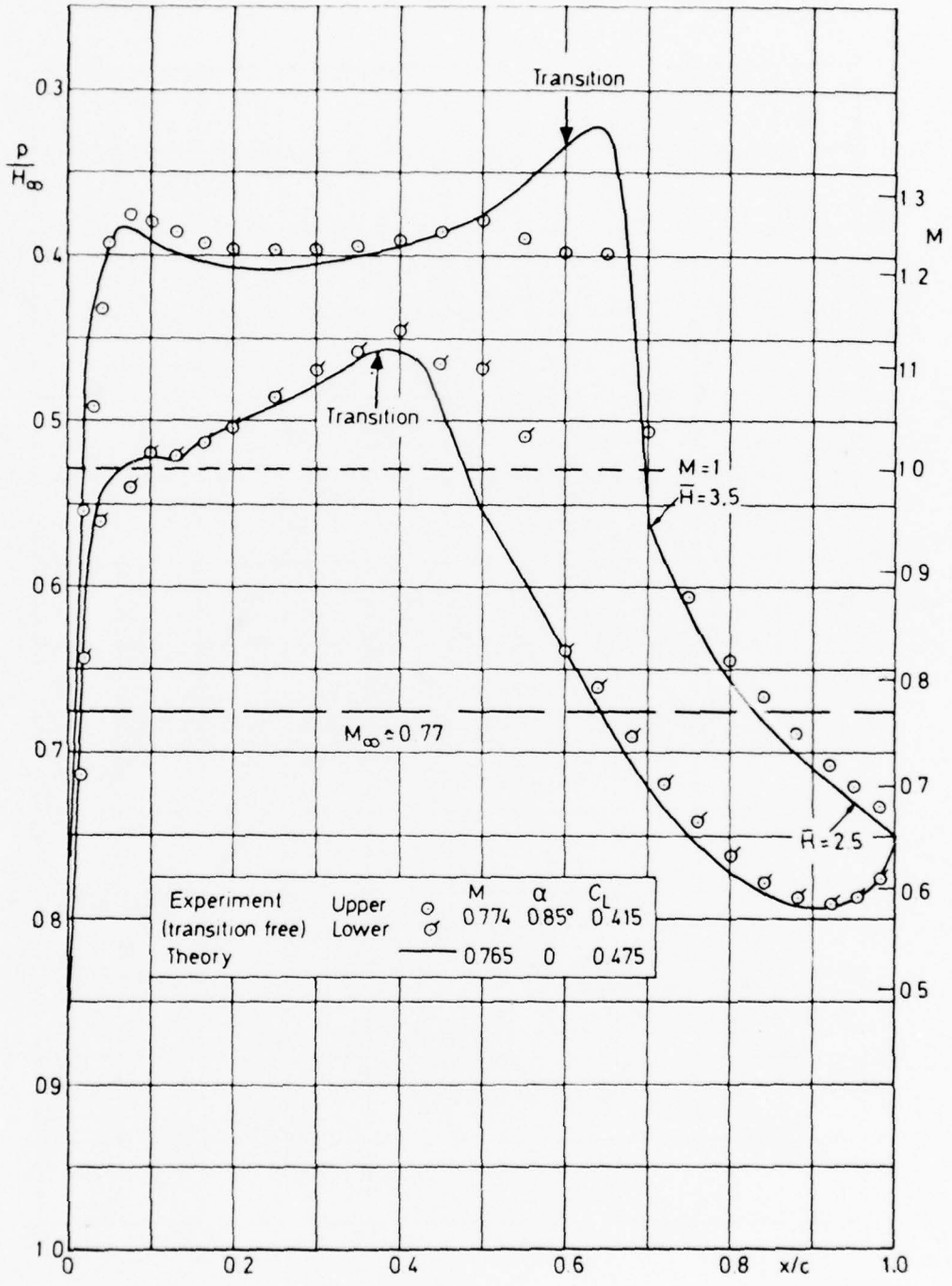

Fig 12 Pressure distributions at $M_\infty \doteq 0.77$, $\alpha_T = 0.85°$

TR 78119

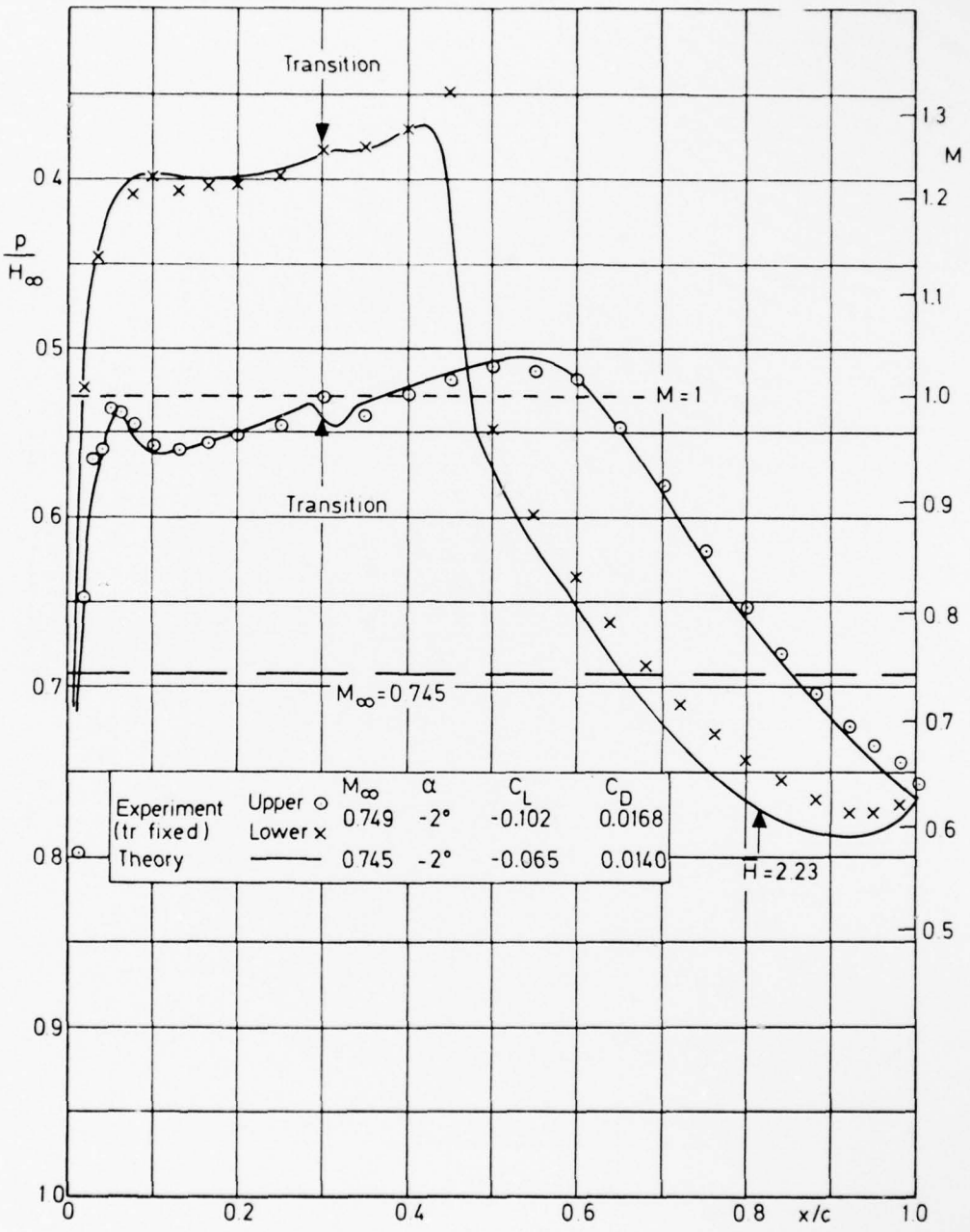

Fig 13 Pressure distributions at $M_\infty \triangleq 0.745$, $\alpha_T = -2°$

TR 78119

Fig 14

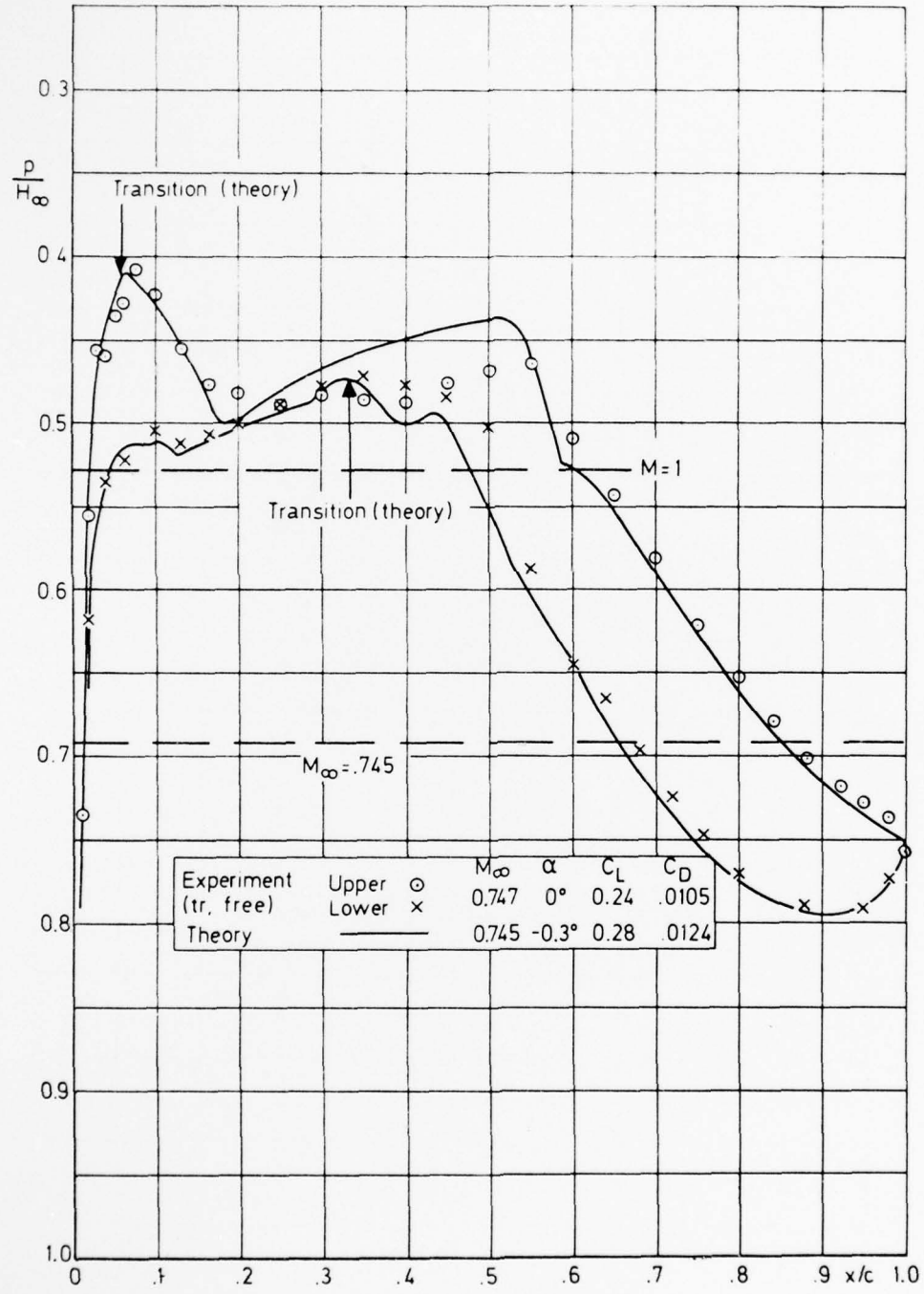

Fig 14 Pressure distributions at $M_\infty \triangleq 0.745$, $\alpha_T = 0$

TR 78119

TR 78119

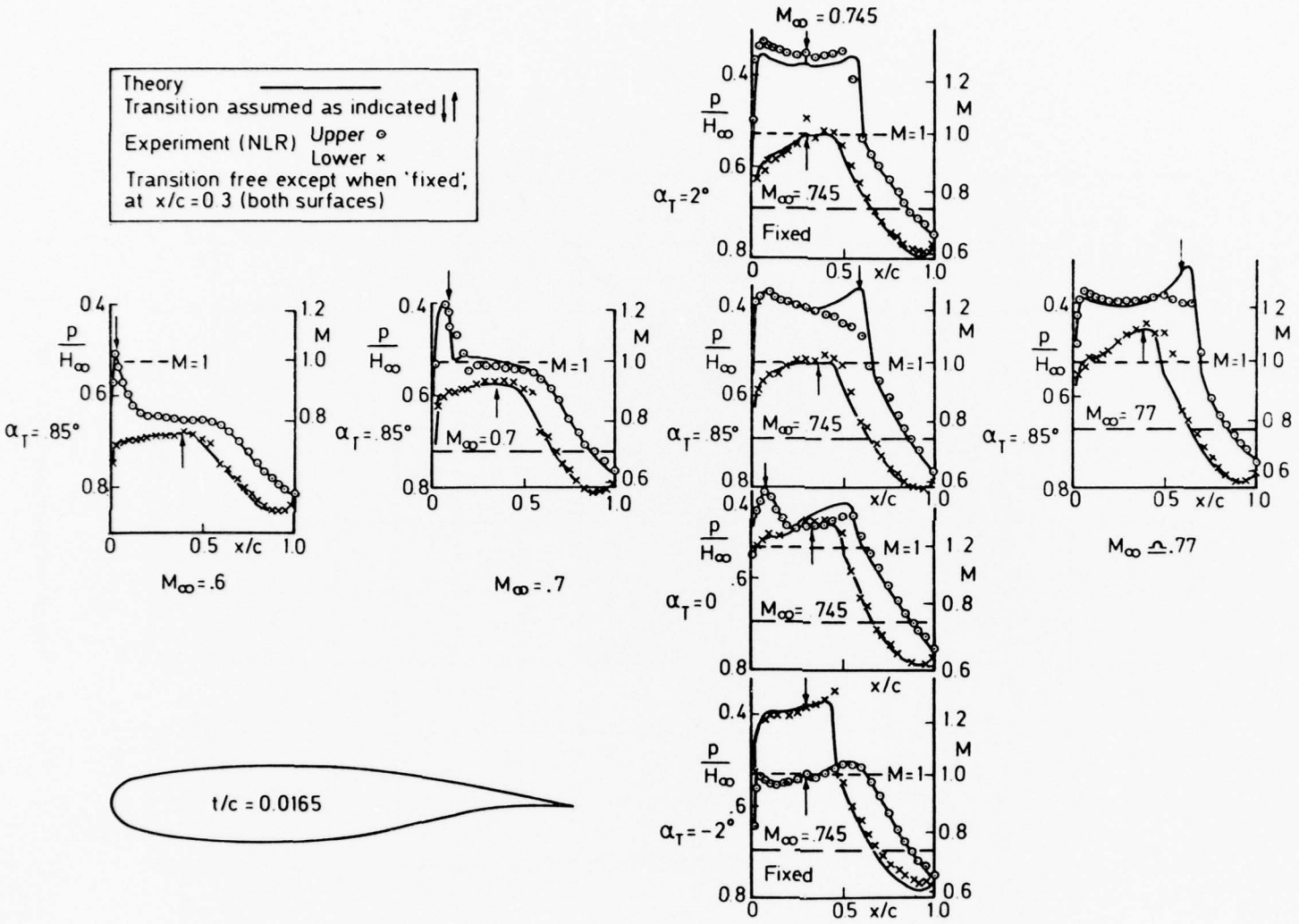

Fig 17 Summary of results at Re ≙ 2.10^6

Fig 17

Fig 18a

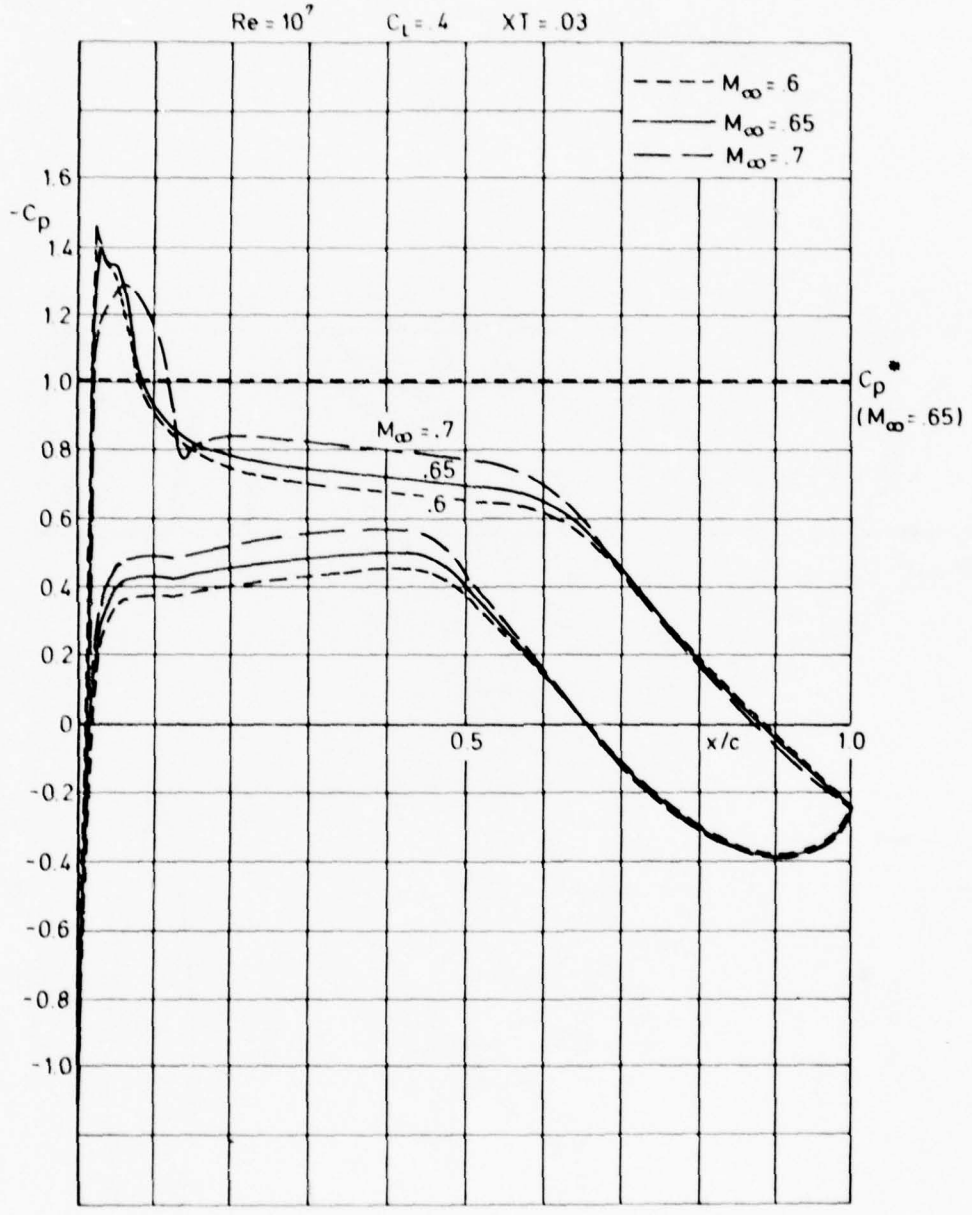

Fig 18a Pressure distributions at $Re = 10^7$, $C_L = 0.4$

TR 78119

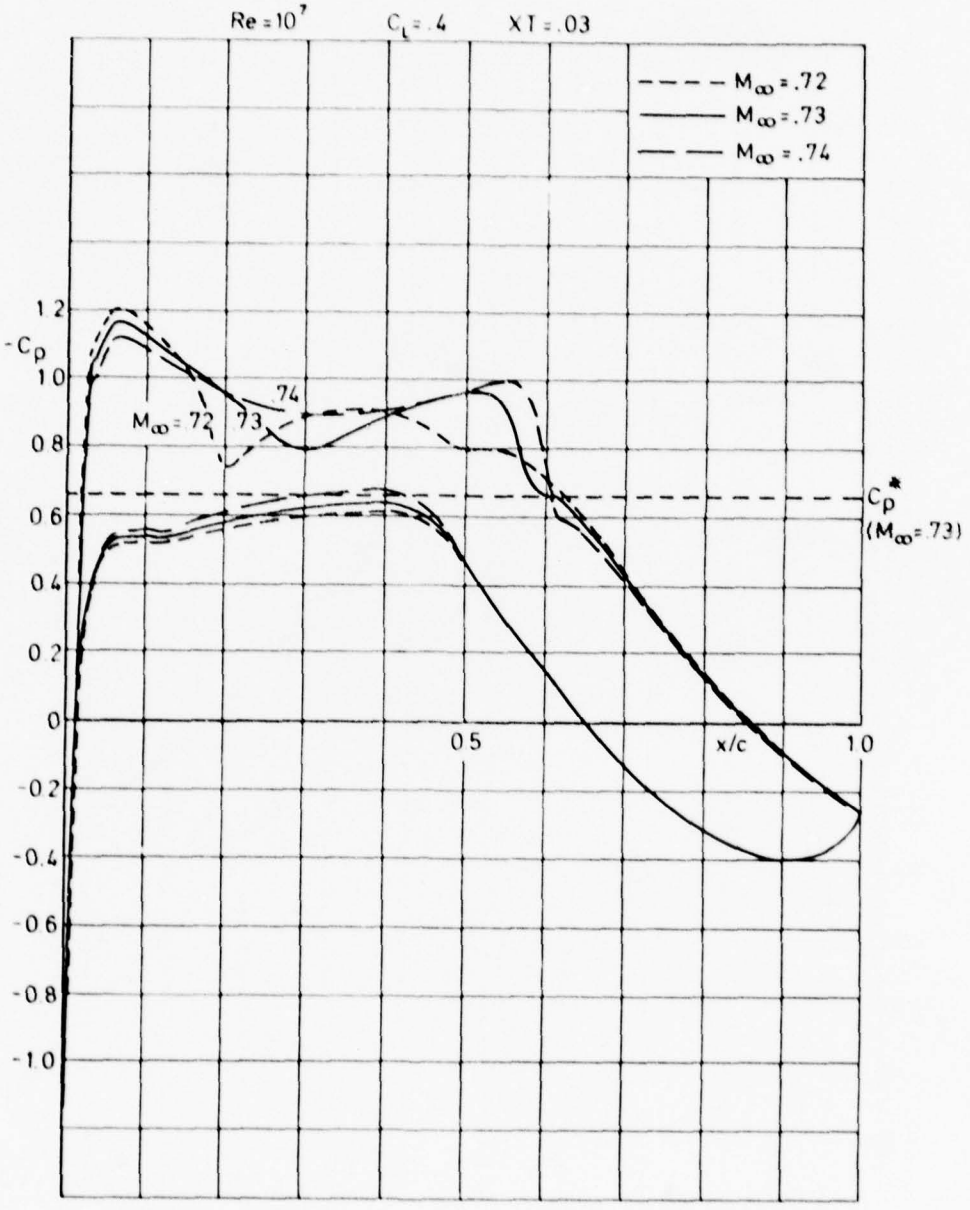

Fig 18b Pressure distributions at $Re = 10^7$, $C_L = 0.4$

Fig 18c

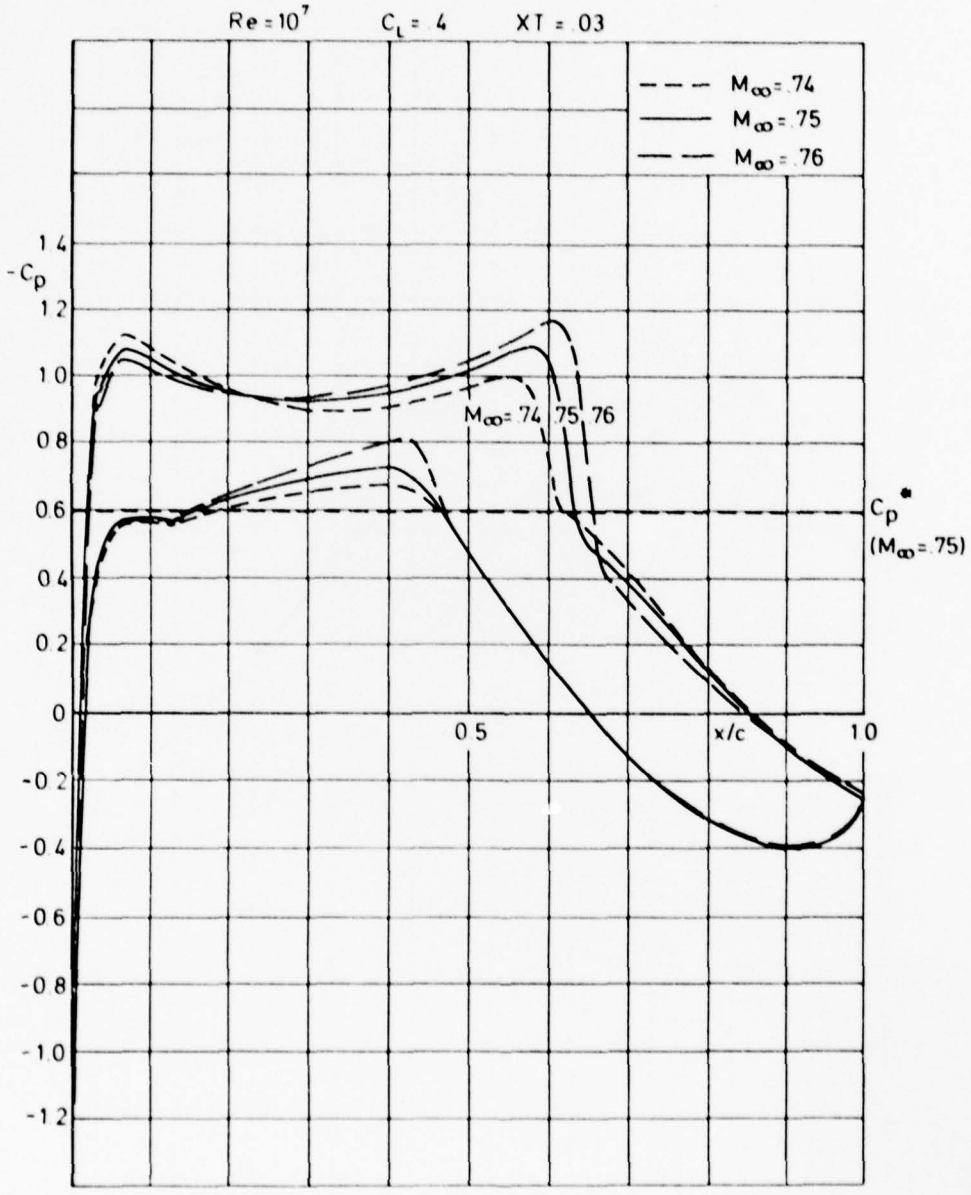

Fig 18c Pressure distributions at $Re = 10^7$, $C_L = 0.4$

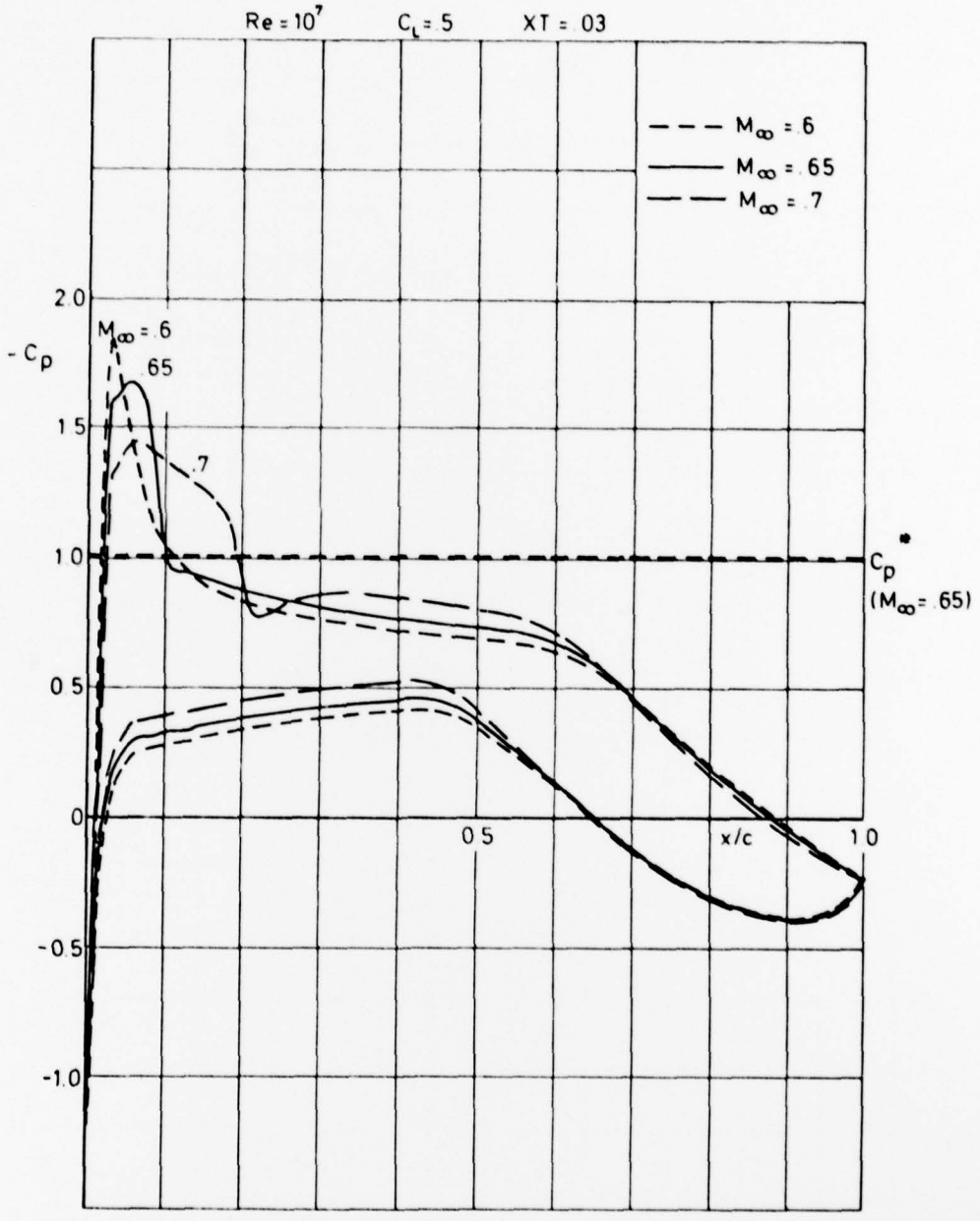

Fig 19a Pressure distributions at $Re = 10^7$, $C_L = 0.5$

Fig 19b

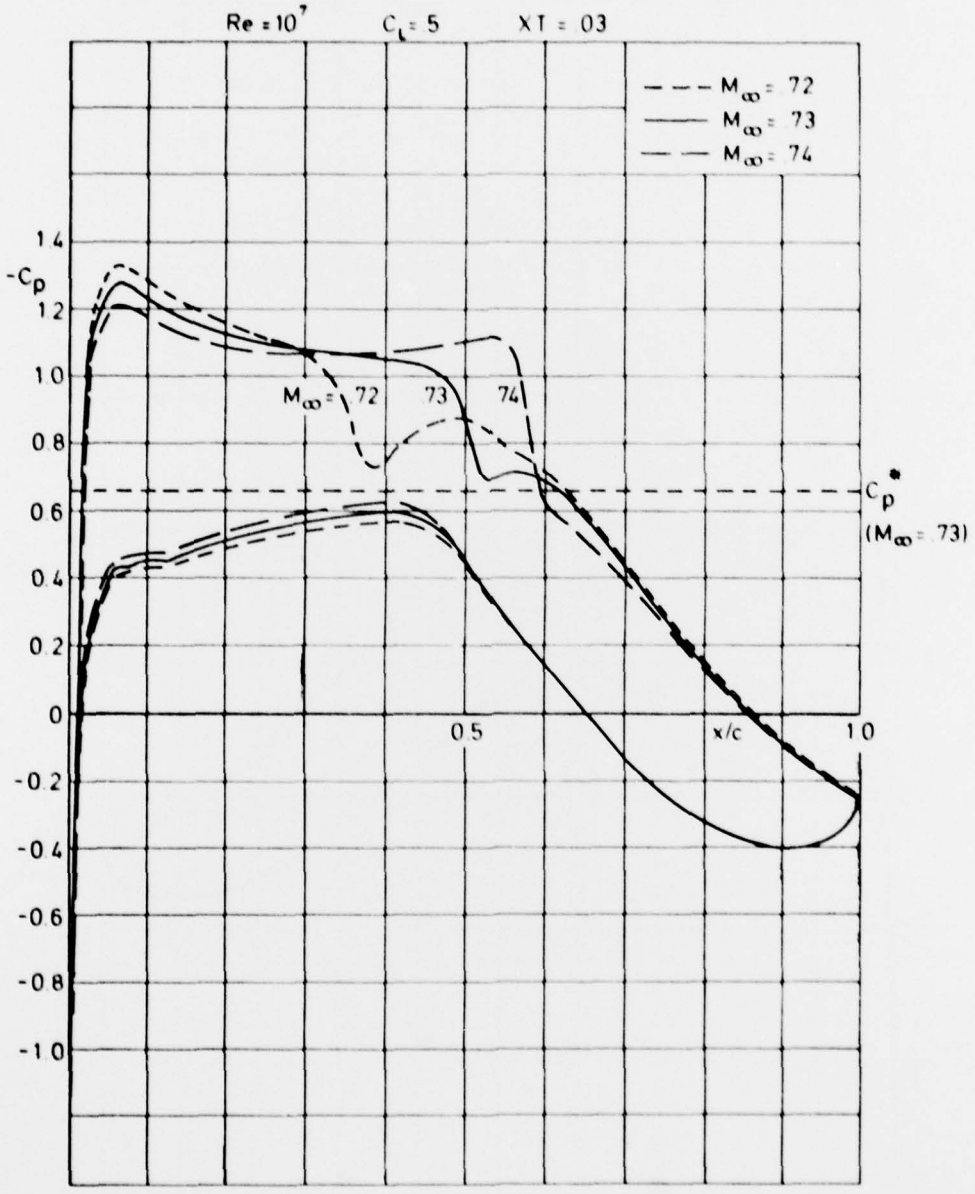

Fig 19b Pressure distributions at $Re = 10^7$, $C_L = 0.5$

Fig 7 Pressure distributions at $M_\infty \triangleq 0.745$, $\alpha_T = 0.85°$

Fig 20a

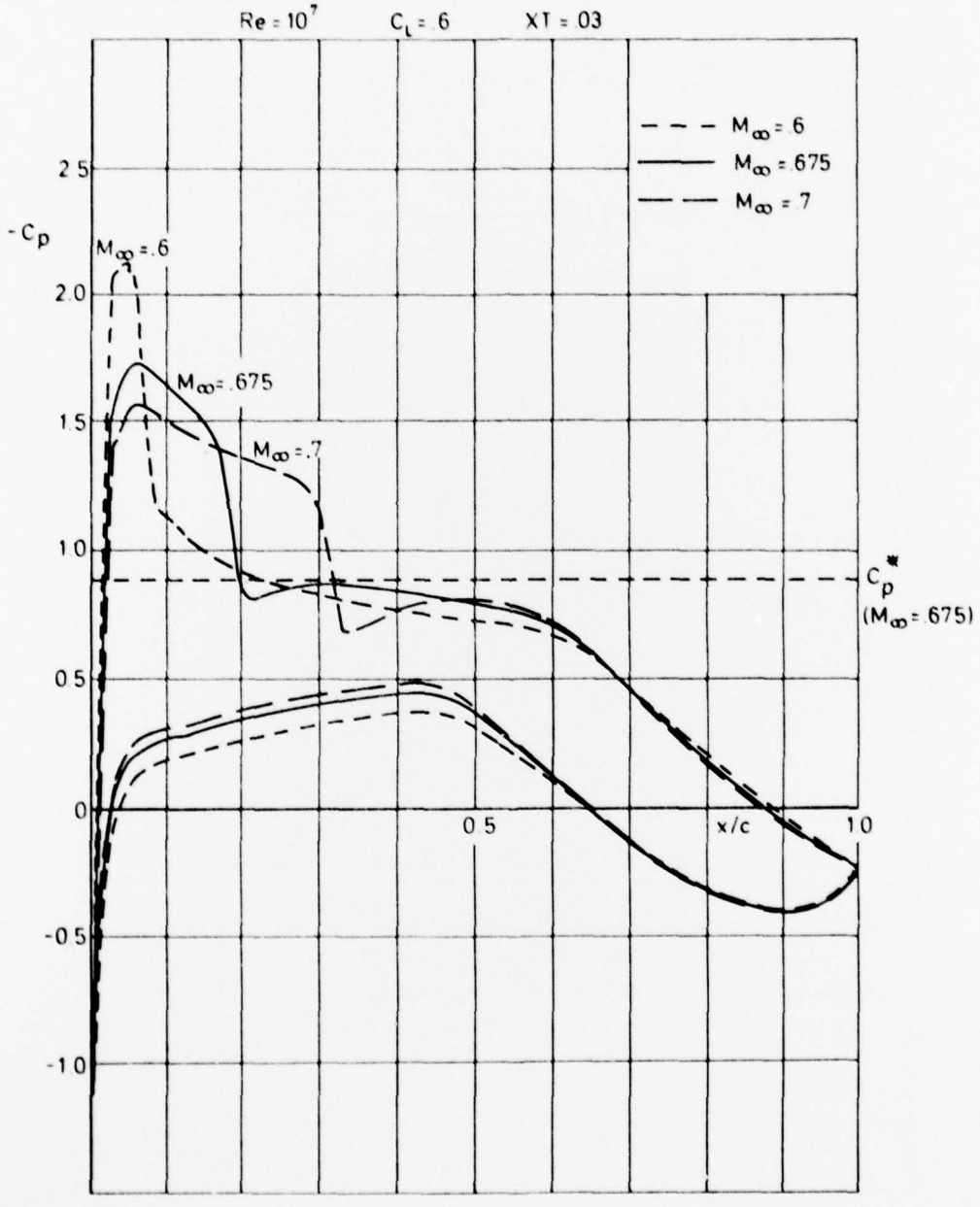

Fig 20a Pressure distributions at $Re = 10^7$, $C_L = 0.6$

Fig 20b

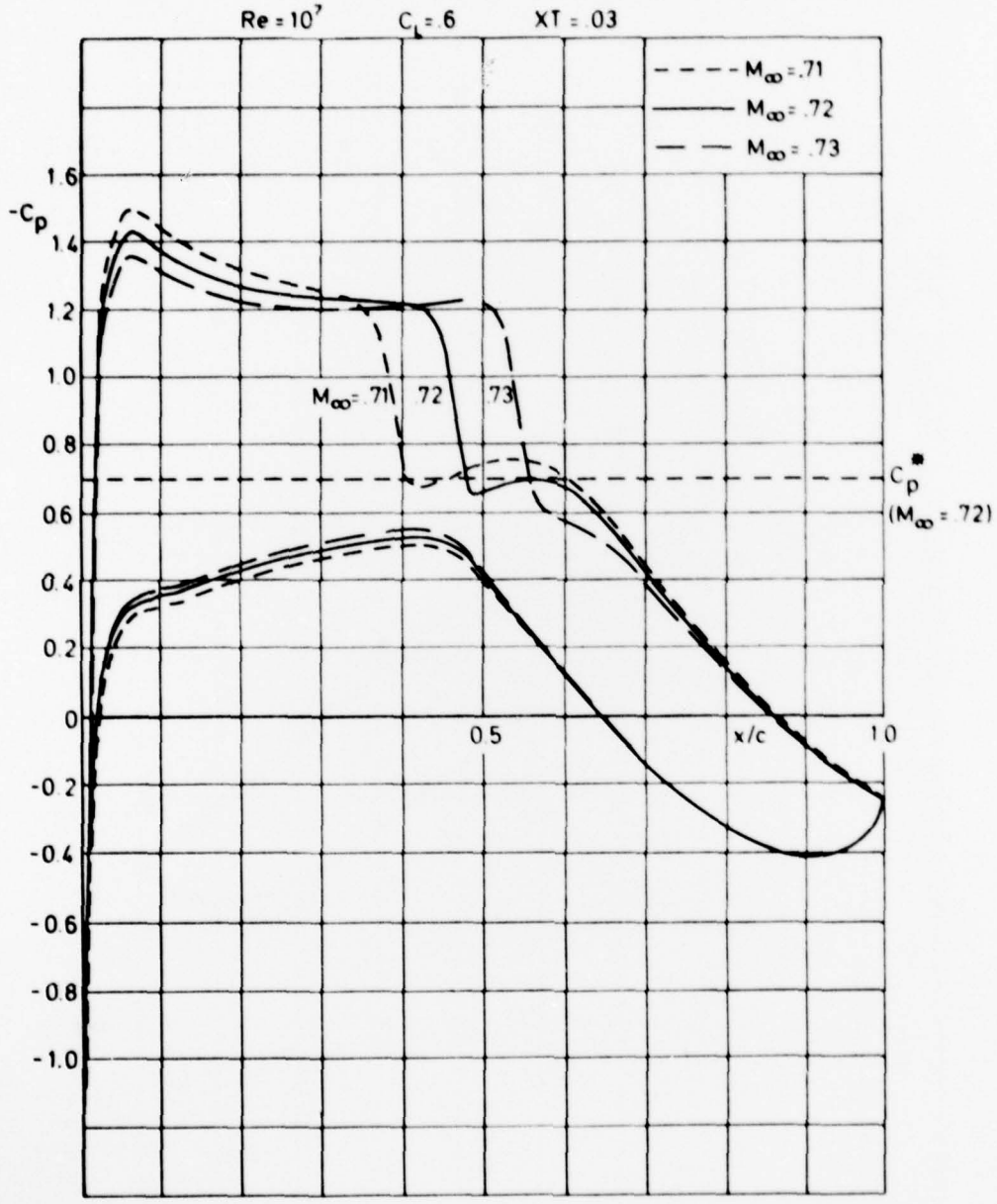

Fig 20b Pressure distributions at $Re = 10^7$, $C_L = 0.6$

TR 78119

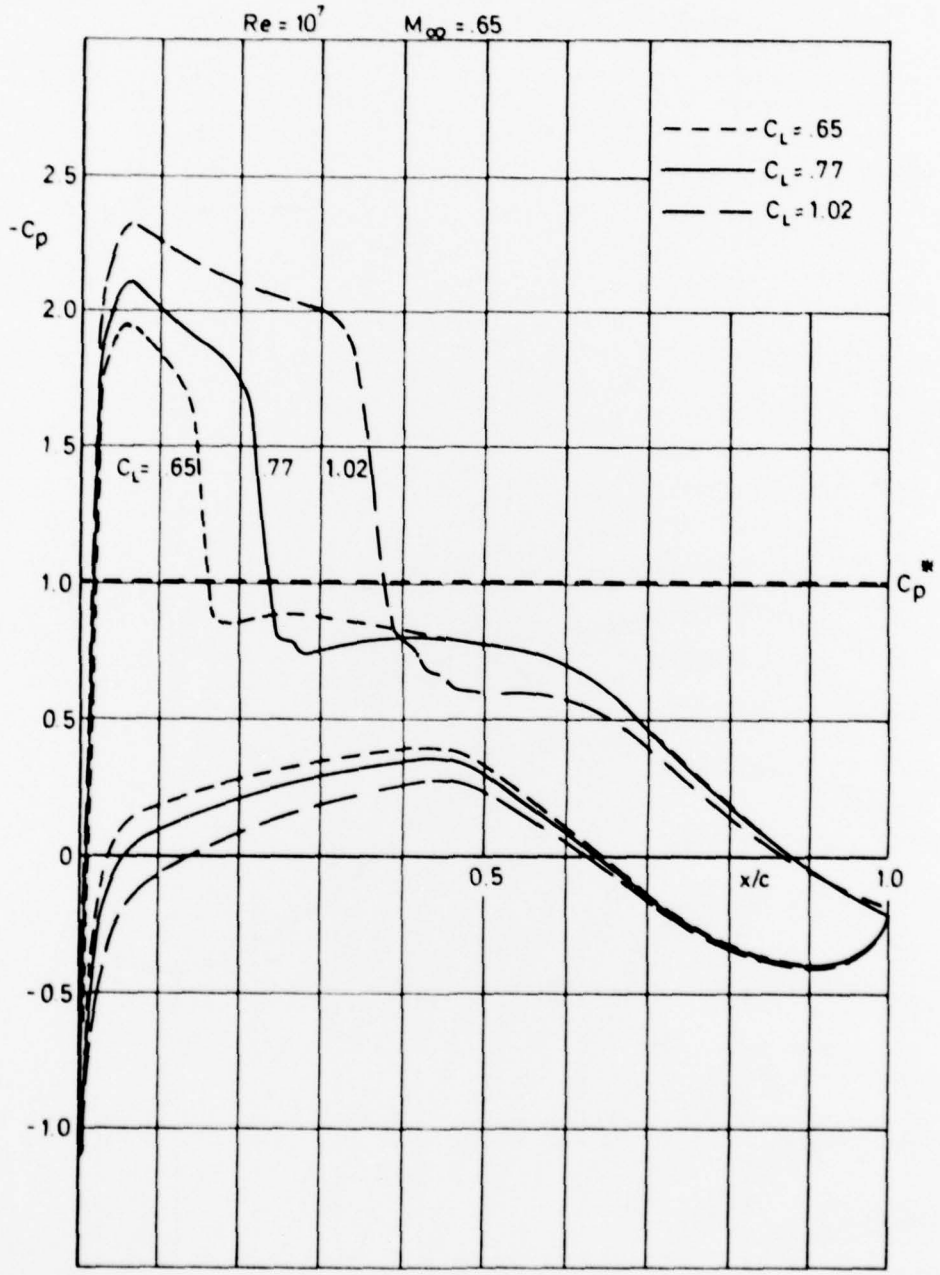

Fig 21 Pressure distributions at $Re = 10^7$, $M_\infty = 0.65$

Fig 22a

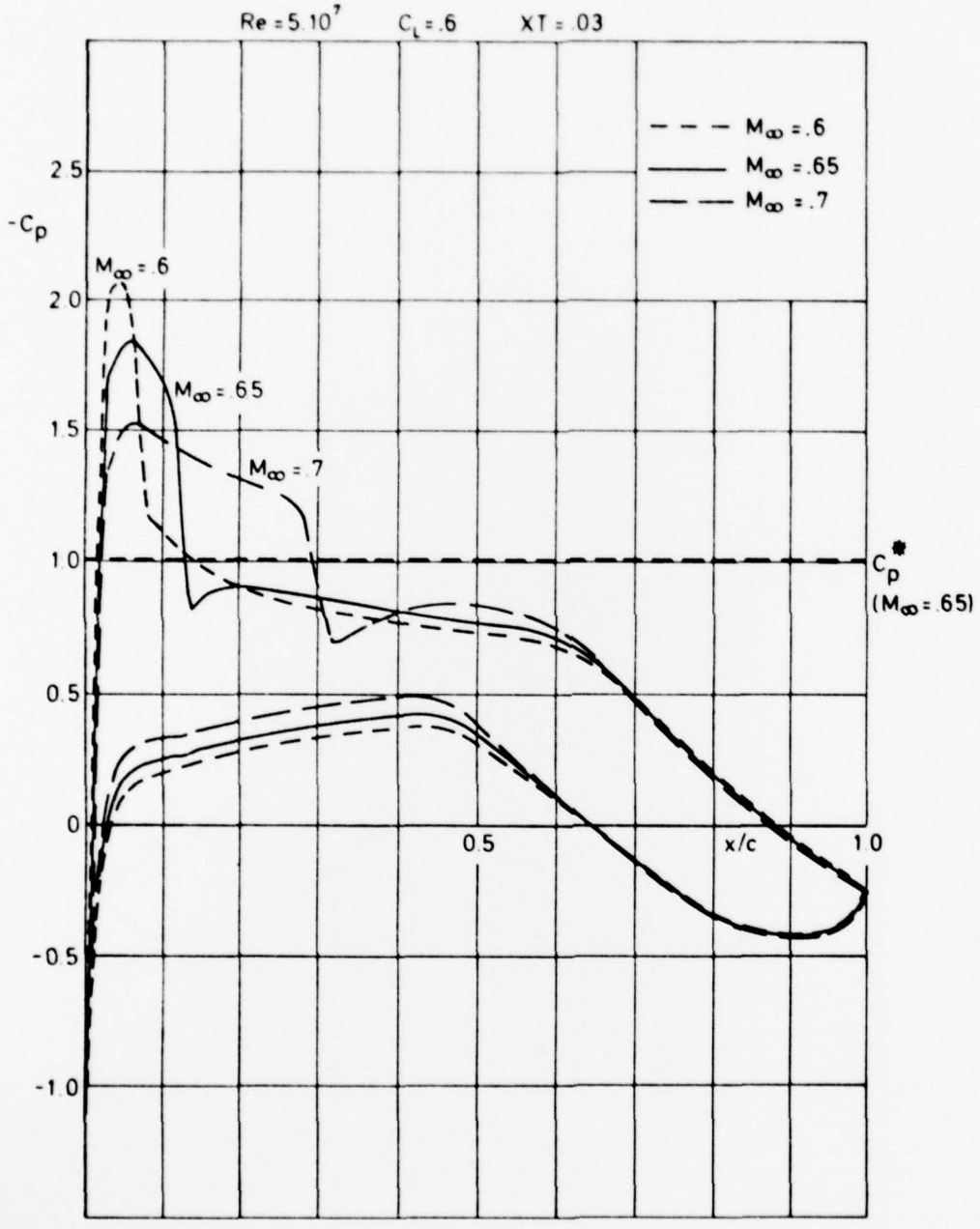

Fig 22a Pressure distributions at $Re = 5.10^7$, $C_L = 0.6$

TR 78119

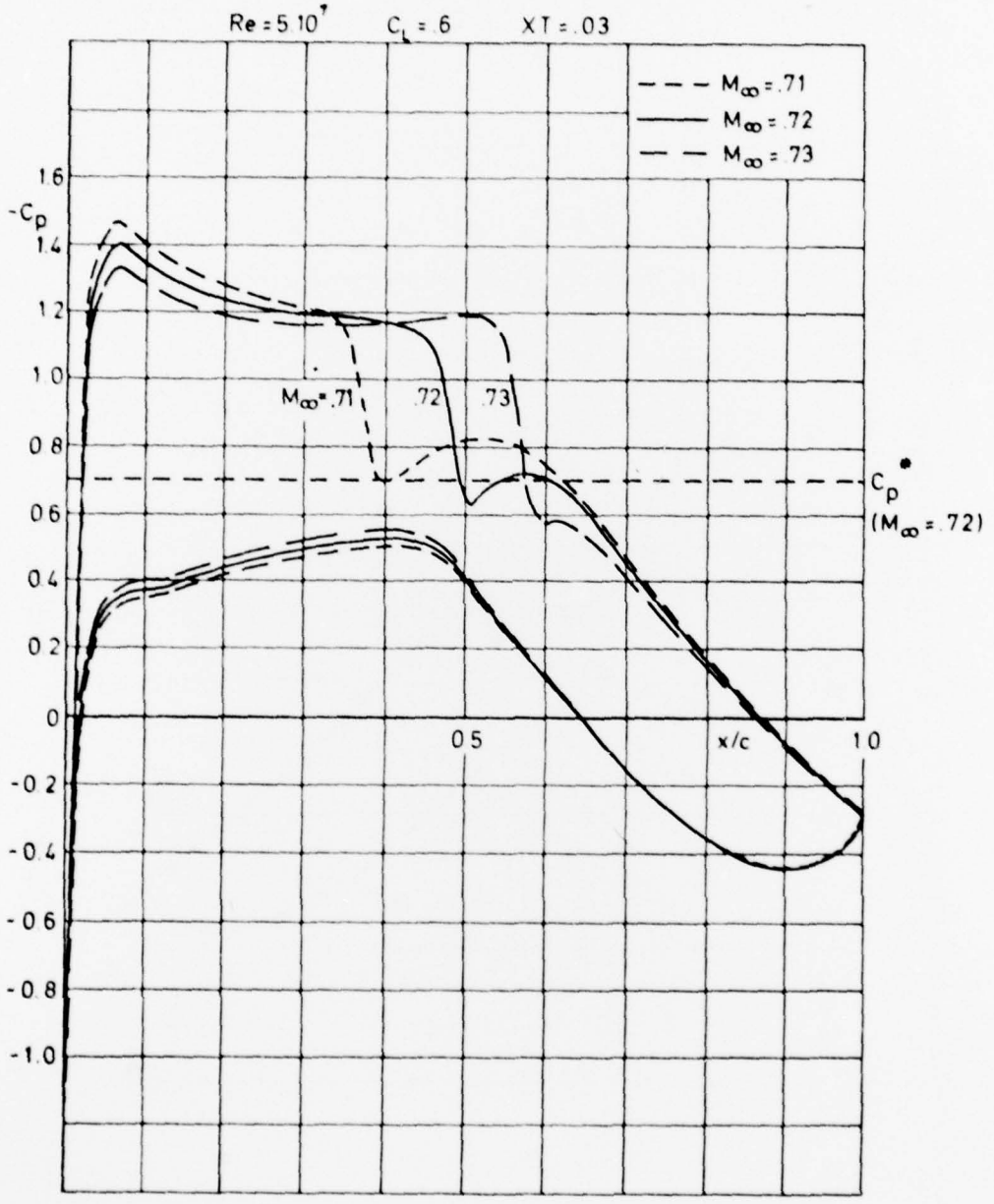

Fig 22b Pressure distributions at $Re = 5.10^7$, $C_L = 0.6$

Fig 23a

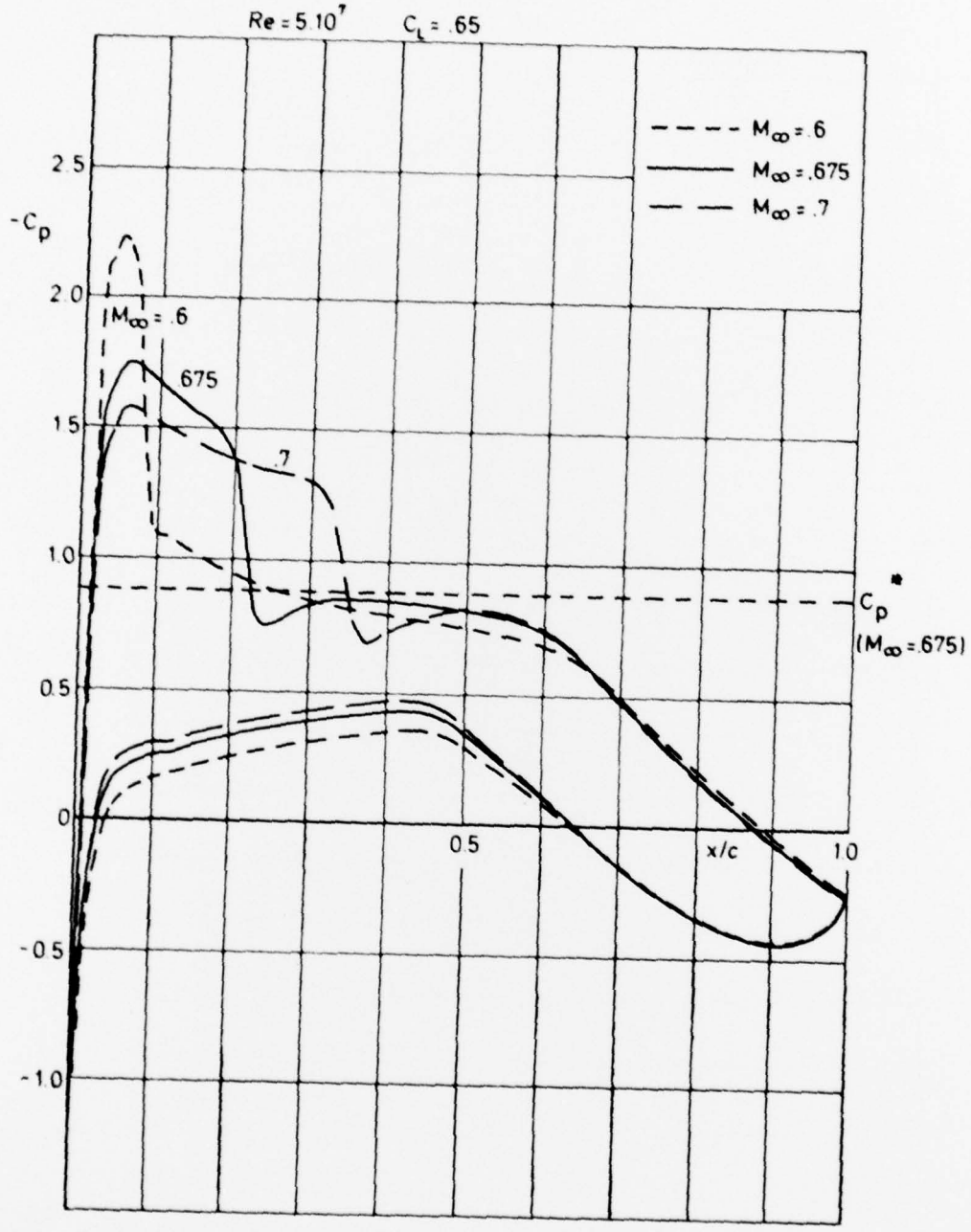

Fig 23a Pressure distributions at Re = 5.10^7, C_L = 0.65

TR 78119

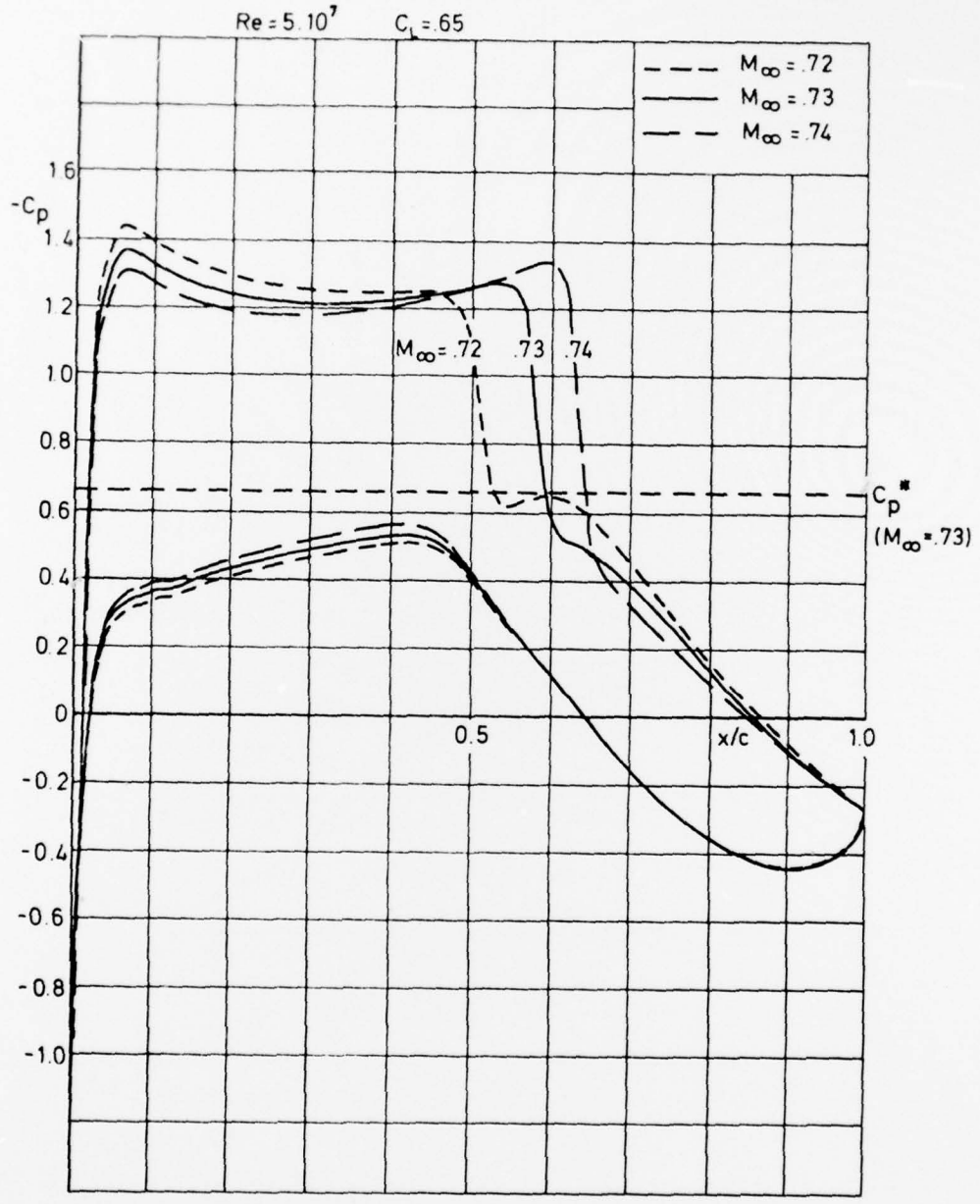

Fig 23b Pressure distributions at $Re = 5.10^7$, $C_L = 0.65$

Fig 24

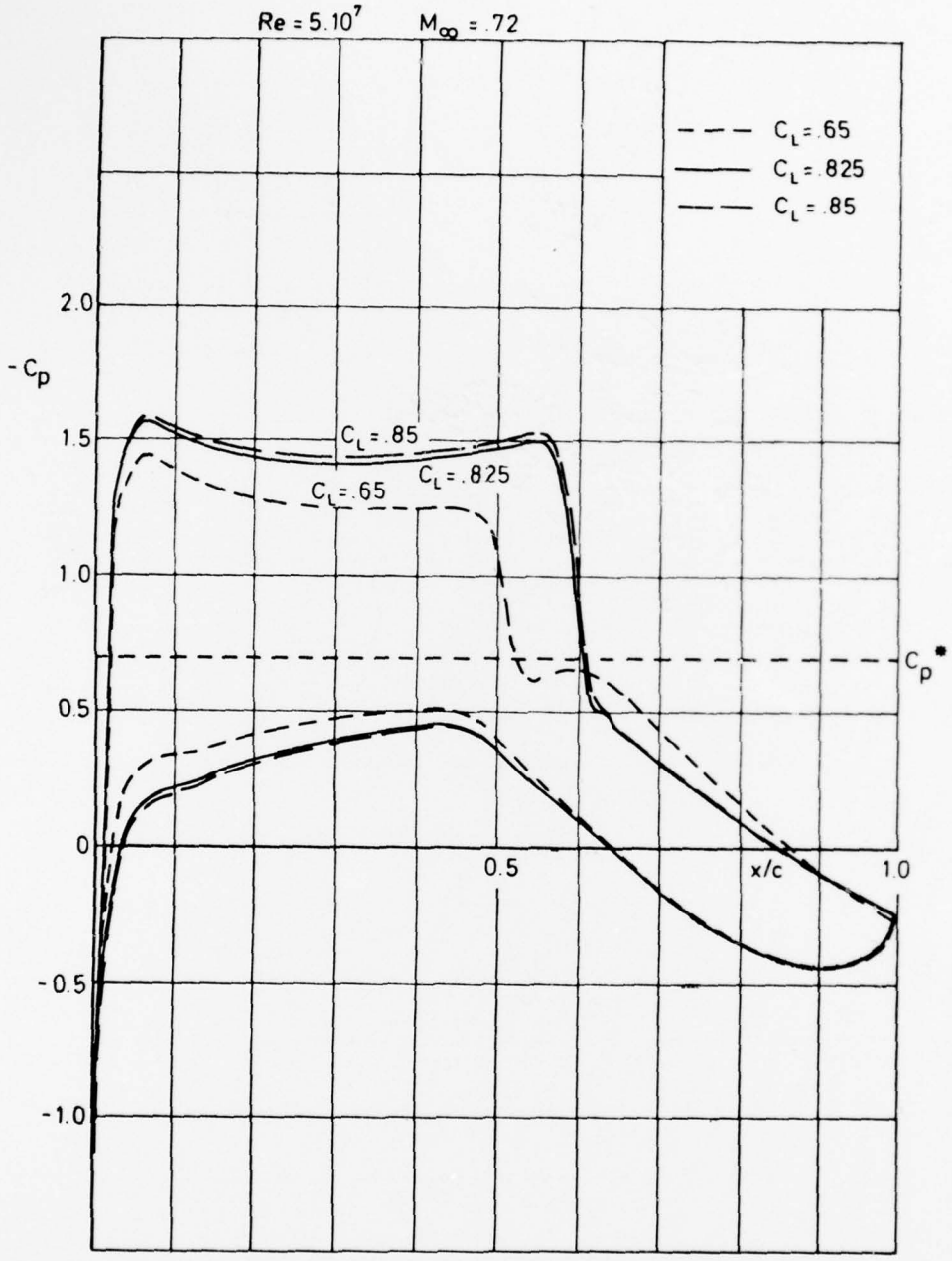

Fig 24 Pressure distributions at $Re = 5.10^7$, $M_\infty = 0.72$

TR 78119

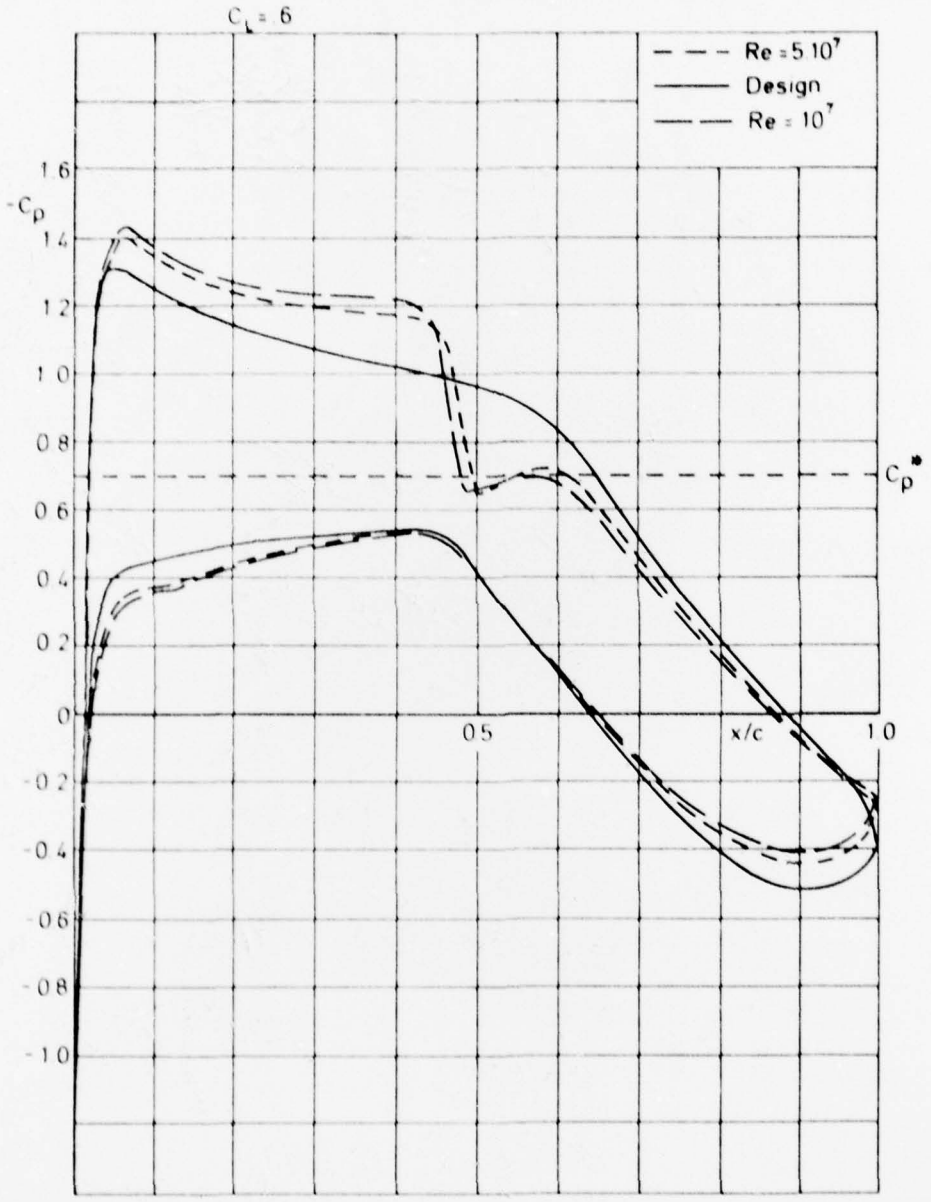

Fig 25 Pressure distributions at $M_\infty = 0.72$, $C_L = 0.6$

Fig 26

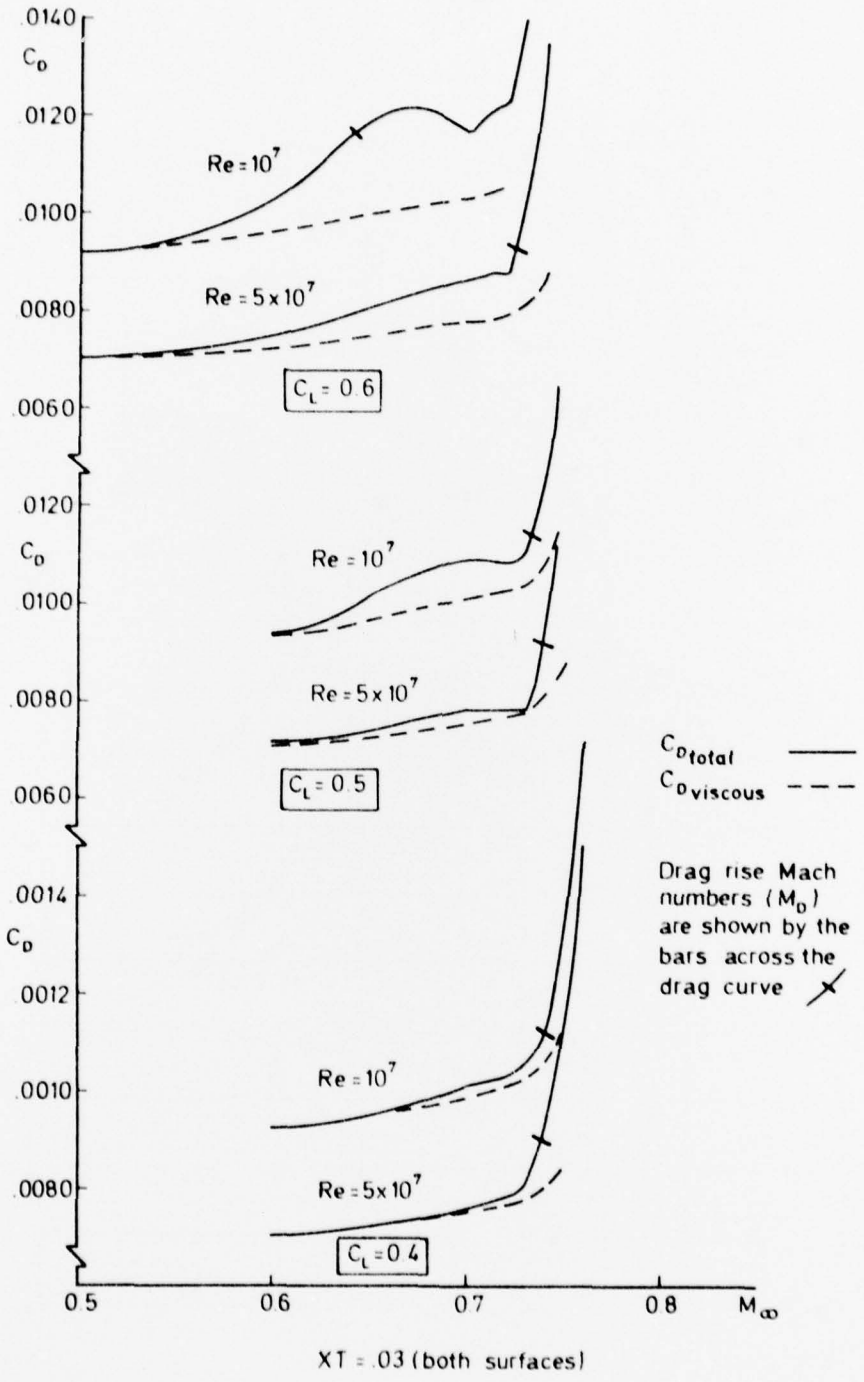

Fig 26 Theoretical drag

TR 78119

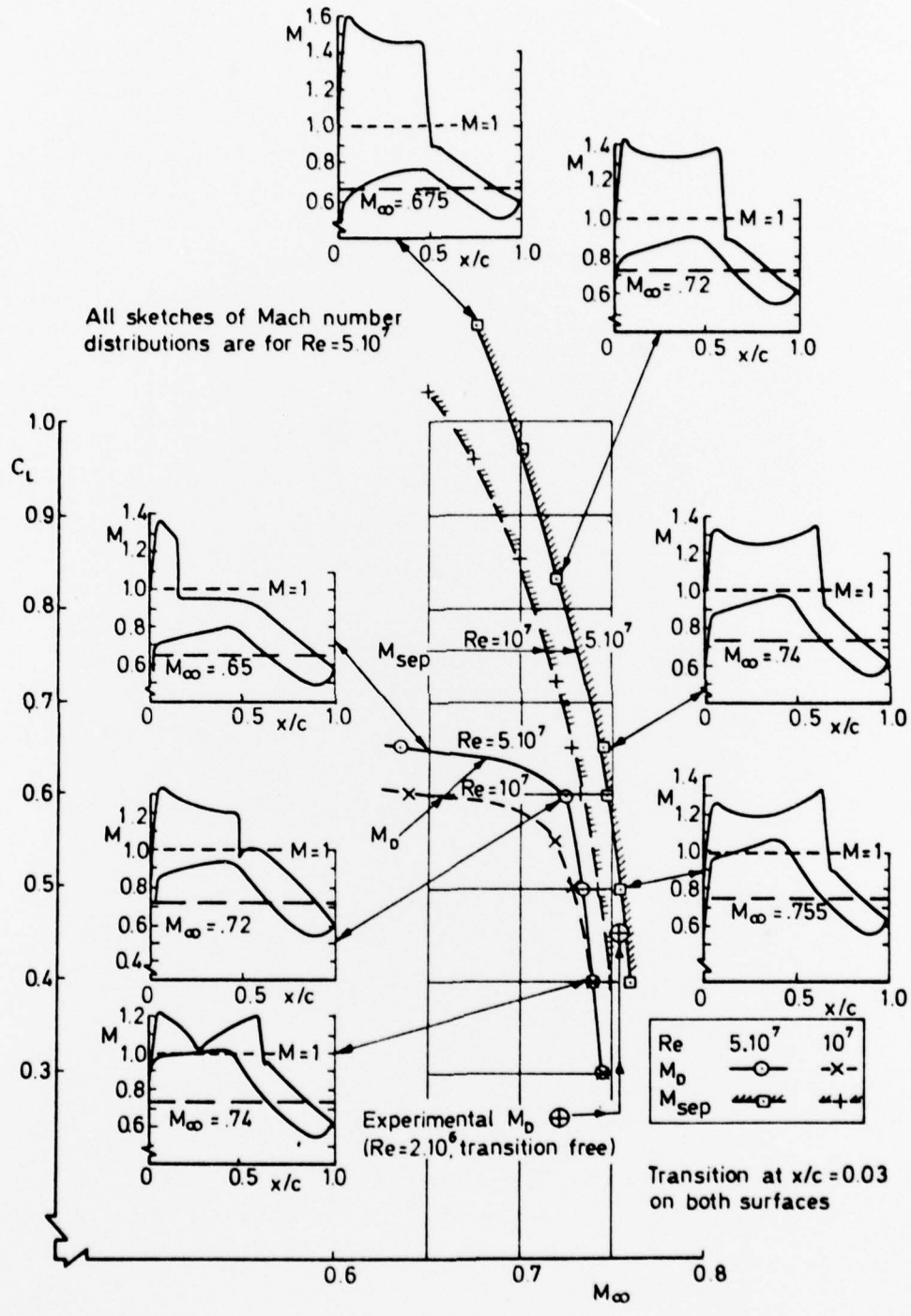

Fig 27 Predicted boundaries for drag rise and separation onset

TR 78119

REPORT DOCUMENTATION PAGE

Overall security classification of this page

UNLIMITED

As far as possible this page should contain only unclassified information. If it is necessary to enter classified information, the box above must be marked to indicate the classification, e.g. Restricted, Confidential or Secret.

1. DRIC Reference (to be added by DRIC)	2. Originator's Reference	3. Agency Reference	4. Report Security Classification/Marking
	RAE TR 78119	N/A	UNLIMITED

5. DRIC Code for Originator	6. Originator (Corporate Author) Name and Location
7673000W	Royal Aircraft Establishment, Farnborough, Hants, UK
5a. Sponsoring Agency's Code	6a. Sponsoring Agency (Contract Authority) Name and Location
N/A	N/A

7. Title A theoretical study of the supercritical aerofoil NLR 7301, and comparison with experiments

7a. (For Translations) Title in Foreign Language

7b. (For Conference Papers) Title, Place and Date of Conference

8. Author 1. Surname, Initials	9a. Author 2	9b. Authors 3, 4	10. Date	Pages	Refs.
Lock, R.C.			September 1978	47	10

11 Contract Number	12. Period	13. Project	14. Other Reference Nos.
N/A	N/A		Aero 3444

15 Distribution statement

(a) Controlled by –

(b) Special limitations (if any) –

16. Descriptors (Keywords) (Descriptors marked * are selected from TEST)

Aerodynamics. Transonic flow. Supercritical aerofoils. Viscous effects.

17. Abstract

The aerofoil NLR 7301, 16.5% thick, was designed at NLR by their generalised hodograph method to give supercritical (inviscid) shock-free flow at the design condition $M_\infty = 0.72$, $C_L = 0.6$. The paper describes a theoretical study of this aerofoil by the latest form of the RAE 'VGK' method for calculating viscous effects in two-dimensional transonic flows. First, comparisons are given with experiments in the NLR Pilot Tunnel at a low Reynolds number (2×10^6). Large discrepancies are shown near the design condition and at higher Mach numbers, which are ascribed to a laminar (transitional) shock wave/boundary layer interaction in the transition-free experiments; this causes an apparent weakening of the shock wave and a spuriously low level of the measured drag. Next, calculations were made at two higher Reynolds numbers, with transition fixed near the leading edge: 10^7, to simulate conditions in a medium-sized wind tunnel; and 5×10^7, typical of full-scale conditions. Favourable scale effects are predicted on drag-rise Mach numbers, for $C_L > 0.5$, and on separation onset at all lift coefficients. It is concluded that the aerofoil should have an excellent performance at high Reynolds numbers.

F5910/1

RAE Form A143